International Journal of Pharmaceutics 586 (2020) 119553

Contents lists available at ScienceDirect

International Journal of Pharmaceutics

journal homepage: www.elsevier.com/locate/ijpharm

Cationic biopolymer functionalized nanoparticles encapsulating lutein to attenuate oxidative stress in effective treatment of Alzheimer's disease: A non-invasive approach

Namdev Dhas, Tejal Mehta*

Department of Pharmaceutics, Institute of Pharmacy, Nirma University, Ahmedabad, Gujarat 382481, India

ARTICLE INFO

Keywords:
Lutein
Core/Shell Nanoparticles
Intranasal delivery
Antioxidant activity
Cell internalization mechanism
Photo and thermal stability

ABSTRACT

Present investigation explores cationic biopolymer core/shell nanoparticles (Chitosan@PLGA C/SNPs) for delivering carotenoids to brain via intranasal route for supressing oxidative stress in Alzheimer's disease (AD). The prepared C/SNPs exhibited particle size less than 150 nm with more than 80% of entrapment efficiency. Surface morphology confirmed uniform coating of shell (chitosan) over core PLGA NPs and suggested spherical nature and homogenous dispersion of C/SNPs. *In-vitro* release study demonstrated sustained release of lutein while C/SNPs permeation enhancement was confirmed by *ex-vivo* diffusion study. The study also investigated effect of cationic-shell with respect to anionic-core NPs on biocompatibility, cellular uptake, uptake mechanism, reactive-oxygen species (ROS) generation, ROS scavenging activity, blood–brain-barrier (BBB) permeation. The cellular uptake revealed enhanced internalization of nanoparticles via caveolae-mediated endocytosis. *In-vitro* co-culture model of BBB demonstrated efficient passage for C/SNPs through BBB. Antioxidant assay demonstrated significant ROS scavenging activity of C/SNPs. *In-vivo* pharmacokinetic and bio-distribution was performed along with *in-vivo* toxicity and stability. *In-vivo* toxicity demonstrated absence of any significant toxicity. Photo and thermal stability confirmed protection of lutein by C/SNPs. C/SNPs were highly deposited in brain following intranasal route. The obtained results demonstrate the potential application of cationic C/SNPs for attenuating oxidative stress in brain for effective AD therapy.

1. Introduction

Alzheimer's disease (AD) is a sub-class of neurodegenerative disease which involves the memory and ognitive capacity loss of patients. Recently, in 2019, Americans with the population of 5.8 million are living with AD. However, at the end of 2050, it has been estimated that 14 million people will be affected. United States Food and Drug Administration (USFDA) has approved several drugs for AD treatment which comes under category, i.e. acetylcholine esterase (AchE) inhibitors viz. rivastigmine, galantamine, tacrine, donepezil and memantine. All the aforementioned drugs are administered orally and were found to be effective in early stage of AD (Dhas et al., 2019). The natural origin flavanoids such as curcumin, rutin, quarcetin, etc. with antioxidant activity have also been utilized to reduce oxidative stress in the treatment of AD. These flavanoids have been explored a lot as an antioxidant agent. Apart from flavonoids, carotenoids are another category of natural origin drug which exhibited antioxidant activity and gained lot of attention of researchers owing to their versatile nature and potential pharmacological activity.

Lutein (LT), a naturally occurring dietary xanthophyll carotenoids obtained from food such as broccoli, corn, egg yolk green vegetables and persimmon. It has anti-oxidant activity; anti-inflammatory activity, anticancer activity and preventing several diseases. LT with its unique structure are prone to heat and light-based degradation and oxidation (Chuacharoen and Sabliov, 2016). Moreover, its applications in the pharmaceutical and food industries have been restricted due to its low solubility, low absorption and low bioavailability (do Prado Silva et al., 2017). Furthermore, implementing the advantages of LT as an antioxidant, it can be utilized to reduce oxidative stress in the treatment of AD. This provokes need to develop its suitable formulation which is devoid of these issues.

The development of specifically designed nanoparticles (NPs) for the transportation of drugs to the brain for AD over the recent few decades has promised an increasingly growing interest in resolving a range of conventional disadvantages of drugs viz. difficulty in passing through blood brain barrier (BBB), lacking ability of targeting specific

* Corresponding author.
E-mail address: tejal.shah@nirmauni.ac.in (T. Mehta).

https://doi.org/10.1016/j.ijpharm.2020.119553
Received 27 April 2020; Received in revised form 12 June 2020; Accepted 13 June 2020
Available online 17 June 2020

site of action, systemic and healthy cell toxicity (Mehta et al., 2019). NP-based delivery platform has attracted lot of attention of researchers owing to its several advantages such as enhanced solubility, reducing dose, reducing dose frequency, brain targeting efficiency through intranasal route.

The intranasal route helps administration of drugs to escape gastrointestinal tract (GIT) and hepatic metabolism. Rich vascularization of nasal mucosa delivers unique characteristics that can increase rate of absorption of drug, following rate of onset of therapeutic effect. Intranasal route can be suitable for the drugs which are unable to permeate through BBB. However, many investigations reported that after intranasal administration, concentration of drug in the brain was found to be low, it may be due to nasal clearance, enzymes present in nasal cavity, patient variability, and acidic environment of nasal region (Piazzini et al., 2019). These drawbacks led to development of potential carrier which can overcome the aforementioned disadvantages.

Amongst several type of NPs such as lipid-based, polymer-based and metal-based NPs, the polymer based core shell NPs (C/S NPs) have shown great potential to be utilized as drug carrier via intranasal route for targeting brain, owing to unique properties viz. biocompatibility, biodegradability, ease of fabrication and cost effectiveness (Dhas et al., 2018). As compared to core NPs alone, C/SNPs can effectively protects drug from external environment-based degradation along with extracellular mechanism such as P-gp efflux, therefore enhancing drug concentration at the site of action (Shah et al., 2016). They can impart tunable and sustained release and better stability as compared to core NPs alone. Amongst several biodegradable polymers, poly (lactic-co-glycolic acid) (PLGA) is an extensively utilized co-polymer owing to its ability to sustain and control the release of drug, biodegradability, biocompatibility and non-toxicity (Khan et al., 2018). Thus PLGA was utilized as a core material in this study. Mucoadhesiveness is important in nasal drug delivery and since the mucin present in the nasal cavity is negatively charged, the positively charged formulation is must to form strong bond formation leading to enhancement of retention time. It has indicated intriguing properties with regards to mucoadhesion, owing to interaction between negatively charged sialic acid present in mucus and positive charged amino groups of chitosan (Islam et al., 2015). Thus, chitosan, a naturally occurring biodegradable cationic polymer was utilized as shell material for coating over the surface of PLGA NPs. Many studies have also investigated that it opens tight junctions and improves the permeation of drugs through the nasal membrane. It also has the ability to absorb water from the mucus layer forming gel-like layer which enhances contact with site of absorption (Abruzzo et al., 2019).

To the best of our knowledge, the application of LT as antioxidant in the treatment of AD using chitosan functionalized PLGA C/SNPs (Chitosan@PLGA C/SNPs) via intranasal route is not explored by researchers till date. In this work, the aim is to develop LT loaded Chitosan@PLGA C/SNPs (Chitosan@LT-PLGA C/SNPs) for intranasal delivery with a view of enhancing stability and bioavailability, reduce cytotoxicity to healthy cells and improve antioxidant activity of LT in treating AD. The PLGA NPs as core was fabricated using nanoprecipitation method. Further, chitosan (as a shell) was coated over the surface of PLGA NPs via electrostatic interaction to form C/SNPs. The optimized NPs were extensively characterized and were further evaluated using various *in-vitro* techniques, and cell line studies viz. *in-vitro*-cytotoxicity, cellular uptake, cellular uptake mechanism, ROS generation study and BBB passage study. *In-vivo* bio-distribution of NPs in various organs was determined after intranasal administration and was performed by conjugating FITC on the surface of NPs. The present research demonstrated the reduction in oxidative stress by use of carotenoids encapsulated C/SNPs following intranasal route.

2. Materials and methods

2.1. Materials and reagents

LT and PLGA (50:50) (MW = 7–17 KDa) were received as a gift sample from Omni Active Health Technologies (Mumbai, India) and Evonik Industries (Essen, Germany), respectively. Low molecular weight chitosan (50–190 KDa) with 75% deacetylation was purchased from Sigma-Aldrich (Bangalore, India). Chloroacetic acid, dialysis membrane (cut-off 12000 Da), Dulbecco's Modified Eagle Medium (F12 Ham DMEM/F12, 1:1 mixture), fetal bovine serum albumin, MTT, L-glutamine, penicillin, streptomycin, isopropyl alcohol, acetone, procured from Himedia (India). Sephadex G-50 was purchased from MPBiomed. All other chemicals were purchased of analytical grade. SHSY5Y human neuroblastoma, RPMI-2650, RAW 264.7, MDCK-II and U-373 MG cell lines were procured from NCCS, Pune, India.

2.2. Fabrication of placebo PLGA NPs and LT-PLGA NPs

Placebo PLGA NPs were fabricated and optimized using nanoprecipitation method as previously reported by Dhas et al. with some modifications (Dhas et al., 2015). In brief, organic phase was prepared by adding PLGA (5 mg/ml) into acetone, whereas, aqueous phase was prepared by adding pluronic-F127 to deionized water (1% w/v). The organic phase was slowly added into aqueous phase (organic: aqueous ratio of 1:6) with a flow rate of 1 ml/ min using a syringe under magnetic stirring at 500 rpm. The stirring was continued for 24 h to remove organic solvent. LT-PLGA NPs were fabricated according to the procedure mentioned above. Along with PLGA, 2 mg LT was also added in organic phase. The unentrapped LT was removed using sephadex column (G-50). LT-PLGA NPs were then lyophilized.

2.3. Preparation of Chitosan@LT-PLGA C/SNPs

Surface functionalization of PLGA NPs was carried out for fabricating C/SNPs using chitosan through electrostatic interaction (Dhas et al., 2015; Piazzini et al., 2019). The PLGA NPs suspension was gently mixed using magnetic stirrer with chitosan solution with various concentrations i.e. 0.01%, 0.02%, 0.03% and 0.04% (w/v).The chitosan concentration and stirring time was optimized through particle size and zeta potential of NPs. Non-reacted chitosan was removed by centrifugation at 10,000 rpm to obtain purified placebo Chitosan@PLGA C/SNPs and Chitosan@LT-PLGA C/SNPs.

All the samples viz. placebo PLGA NPs, placebo Chitosan@PLGA C/SNPs, LT-PLGA NPs and Chitosan@LT-PLGA C/SNPs were lyophilized using 5% mannitol (cryoprotectent) in lyophilizer at −70 °C for 12 h.

2.4. Entrapment efficiency (EE) and drug loading (DL)

The entrapment efficiency of LT in the LT-PLGA NPs and Chitosan@LT-PLGA C/SNPs was determined using sephadex column. The LT-PLGA NPs and Chitosan@LT-PLGA C/SNPs were successfully passed through the sephadex column whereas the un-entrapped LT was blocked in the column which was collected by passing LT soluble solvent. LT was estimated using DMSO: methanol (1:9) in UV-spectrophotometer at λmax of 446 nm. The experiments were performed in triplicate. The %EE and %DL were determined using following equations (Equation (1) and (2)) (Alhakamy and Md, 2019).

$$\%EE = \frac{AmountofLTinNPs}{TotalamountofLTadded} * 100 \quad (1)$$

$$\%DL = \frac{AmountofLTentrappedinNPs}{Totalweightofformulation} * 100 \quad (2)$$

2.5. Characterization of prepared NPs

The determination of particle size, particle distribution and surface charge of prepared NPs were analysed by photon correlation spectroscopy using zetasizer (Horiba SZ-100 Nanopartica, 2 Miyanohigashi, Kisshoin Minami-ku, Kyoto, Japan). The particle size and PDI measurement was performed at 90^0 of detection angle at 25 °C after suitable dilutions in double-distilled water. The zeta potential of NPs dispersed in double-distilled water was measured on the basis of electrophoretic mobility under an electric field with an average of 25 measurements. The Fourier transform infra-red spectrum of prepared NPs was analysed in the wavenumber range of 400 to 4000 cm^{-1} using FTIR (FTIR spectrometer, IR Affinity- 1S (Shimadzu, Japan). pXRD patterns were analysed using X-ray diffractometer (Ultima IV, Rigaku) in the range of 5 to 50 (2θ value) to determine the degree of crystallinity and incorporation of LT into PLGA NPs and chitosan@PLGA C/SNPs. Transmission electron microscopy ((TEM) (Philips-CM 200)) was utilized for observing the morphology of formulated PLGA NPs and Chitosan@PLGA C/SNPs. Briefly, 20 µl of LT-PLGA NPs and Chitosan@LT-PLGA C/SNPs dispersion was put on copper grid coated with carbon film and air dried. Then phosphotungstic acid was added to stain PLGA NPs and Chitosan@PLGA C/SNPs negatively and allow to stand for 5 min after that observed with magnification between 25x and 75000x.

2.6. In-vitro drug release profile

In-vitro release of LT from LT suspension, LT-PLGA NPs and Chitosan@LT-PLGA C/SNPs was determined using dialysis membrane diffusion method (Sawant et al., 2016). Briefly, the known amount of lyophilized NPs suspension (equivalent to 2 mg of LT) was added into dialysis bag. Later, each dialysis bags containing LT suspension, LT-PLGA NPs and Chitosan@LT-PLGA C/SNPs suspension; were suspended in beaker containing 100 ml of phosphate buffer (pH 7.4) containing 0.5% tween 80; stirred at constant speed of 100 rpm and maintained at 37 ± 2 °C. Aliquots were collected at fixed time intervals from the medium outside the dialysis bag. The medium was immediately replaced with equal volume i.e. 0.5 ml of fresh phosphate buffer to maintain sink condition. The LT concentration was measured using UV spectrophotometer at 446 nm. The experiment was performed in triplicate.

2.7. Ex-vivo diffusion profile

Ex-vivo diffusion investigation of LT suspension, LT-PLGA NPs and Chitosan@LT-PLGA C/SNPs were conducted with the help of freshly excised goat nasal mucosa using franz-diffusion cell (Sawant et al., 2016; Venkateswarlu and Manjunath, 2004). Briefly, nasal mucosa was placed between acceptor and donor compartment. Acceptor compartment was filled with 25 ml of phosphate buffer (pH 7.4) containing 0.5% tween 80. Donor compartment was filled with 2 ml of LT suspension (2 mg/ml), LT-PLGA NPs and Chitosan@LT-PLGA C/SNPs with 4 mg equivalent weight of LT in the NPs. Aliquots were collected at fixed time intervals from the receptor compartment and was replaced with equal volume of freshly prepared phosphate buffer containing 0.5% tween 80. The LT concentration was measured using UV spectrophotometer at 446 nm. The experiments were performed in triplicate.

2.8. Estimation of cellular uptake

Quantitative analysis of cellular uptake of FITC, FITC conjugated placebo PLGA NPs, FITC conjugated placebo Chitosan@PLGA C/SNPs, FITC conjugated LT-PLGA NPs and FITC conjugated Chitosan@LT-PLGA C/SNPs was investigated in SH-SY-5Y cell line using spectrofluorometer (Meng et al., 2018). Briefly, the SH-SY-5Y cells were seeded in 6-well plate at a density of $5*10^5$ cells/ well and incubated under 5% CO_2 environment at 37 °C for 24 h. The cells were further incubated with same concentration of various samples mentioned above, for 2 h at 37 °C and subsequently washed 3 times with the help of PBS. Later on, post-removal of the supernatant, cells were trypsinized and centrifuged for 5 min at 1500 rpm to obtain cell pellets. Further, cells were re-suspended in PBS followed by analysis using spectrofluorometer and the cellular uptake-related fluorescence intensity was measured.

Qualitative cellular internalization analysis of FITC conjugated LT-PLGA NPs and FITC conjugated Chitosan@LT-PLGA C/SNPs were performed using fluorescence microscopy in SH-SY-5Y cells. In brief, both the NPs were exposed to SH-SY-5Y sub-confluent culture for 4 h respectively. The cells were then washed and fixed with the help of 1% paraformaldehyde and images were taken on Zeiss LSM 510 confocal microscope (Germany) (excitation wavelength = 488 nm, emission wavelength = 560 nm)

2.9. Cell uptake mechanism

Cell entry mechanism was investigated using SH-SY-5Y cell line and measured spectrofluorometer. The study involves several endocytic inhibitors viz. chlorpromazine (receptor and clathrin-mediated endocytosis inhibitor), nystatin (lipid raft/caveolae-mediated endocytosis inhibitor) and sodium azide (macropinocytosis-based endocytosis inhibitor) (Pandey et al., 2019). Briefly, SH-SY-5Y cells were seeded on 6-well plate at density of $5 *10^5$ cells/wells. Further, cells were pre-incubated for 1 h at 37 °C with different endocytic inhibitors at the following concentrations: chlorpromazine (10 µg/ml), nystatin (50 µg/ml) and sodium azide (0.1% w/v). After this pre-incubation, FITC conjugated placebo PLGA NPs, FITC conjugated placebo Chitosan@PLGA C/SNPs, FITC conjugated LT-PLGA NPs and FITC conjugated Chitosan@LT-PLGA C/SNPs were added and incubated for next 2 h. The cells were then washed three times with PBS followed by lysis of cells using Triton X-100 (1%) and analysed using spectrofluorometer. The cells when exposed to only individual NPs were considered as control and their uptake is designed as 100%.

2.10. In-vitro cell viability assay

In-vitro cell viability assay of various samples viz. pure LT, placebo PLGA NPs, placebo Chitosan@PLGA C/SNPs, LT-PLGA NPs and Chitosan@LT-PLGA C/SNPs was evaluated using MTT assay against SH-SY-5Y and RPMI 2650 cell lines (Tang et al., 2019). Briefly, cells were seeded on 96 well cell culture plates at a density of $1*10^4$ cells/well and left for seeding 24 h at 37 °C with 5% CO_2. All samples with different concentration i.e. 10–50 µg/mL were exposed to both SH-SY-5Y and RPMI 2650 cell lines for 24 h. Later the culture media was removed from each well plate and replaced with MTT solution with concentration of 5 mg/ml at 37 °C for 4 h. The medium was removed after incubation and then 150 µl of DMSO was utilized to dissolved formed formazan crystals, followed by absorbance of formazan reduction product using spectrophotometer at 570 nm using microplate reader (BioRad). The experiments were performed in triplicate.

2.11. Generation of ROS

ROS generation study was carried out using RAW 264.7 cells (Paka and Ramassamy, 2017). The cells were seeded in 96 well-plate with the density of $2*10^4$ cells/well for 24 h. The samples viz. pure LT, placebo PLGA NPs, placebo Chitosan@PLGA C/SNPs, LT-PLGA NPs and Chitosan@LT-PLGA C/SNPs were then added into the cells with various concentrations (10, 20, 30, 40 and 50 µg/ml) in presence of 10 µg/ml of H_2O_2. The ROS was measured by incorporating H2DCFDA to sample treated cells and observed signal generated from oxidized form (dichlorofluorescein; DCF) at 535 nm using microplate reader. The experiments were carried out in triplicate. The ROS generated was expressed as a ratio of the fluorescence of DCF of treated cells to that of

untreated cells

2.12. In-vitro BBB permeation study

The NPs ability to permeate through BBB was investigated as described by Pandey et al. using cellular in-vitro model of BBB (Pandey et al., 2019). Co-culture model was developed by seeding U-373 MG cells with density of 7.5* 10^4 cells per well on apical side of insert (Corning, New York) which was coated with gelatin solution (2% w/v) and permitted to grow for 30 min. The inserts were then placed into 12 well plates containing DMEM and incubated for 24 h at 37 °C. Later, seeding of MDCKII cells with a density of 150*10^4 cells per well was carried out at inner side of inserts and were incubated for 24 h at 37 °C. Further, samples viz. pure LT, LT-PLGA NPs and Chitosan@LT-PLGA C/SNPs were diluted with serum free DMEM and were then added to luminal chamber of inserts at concentration of 1 ml/well (2 mg/ml). Later, withdrawal of 200 µl of medium at different time points i.e. 0, 2, 24, 48 h, was carried out from basal chamber. Equal amount of serum free DMEM was added into basal chamber to maintain sink condition. The permeation of pure LT, LT-PLGA NPs and Chitosan@LT-PLGA C/SNPs was measured using spectrofluorometer and transport ratio was calculated using formula,

$$transportratio(\%) = \frac{Az}{A} * 100 \quad (3)$$

Where, Az indicates amount of LT in basal chamber at zth h (2, 24, 48 h) and A indicates the amount of LT added in apical chamber.

2.13. Evaluation of antioxidant enzyme activity

The antioxidant assay was performed using superoxide dismutase (SOD), monoldialdehyde (MDA) and catalase (CAT) activity-based assay. The RAW 264.7 cell line was utilized for determining the antioxidant activity of prepared samples. The samples viz. pure LT, LT-PLGA NPs and Chitosan@LT-PLGA C/SNPs with different concentrations (0, 5, 10, 20 mM) were exposed to RAW 264.7 cells for 20 h. The positive control group and pure LT, LT-PLGA NPs and Chitosan@LT-PLGA C/SNPs-treated groups were then exposed to 500 µM of H2O2 for 8 h, respectively (Lin et al., 2019). The SOD, MDA and CAT activity in cell was measured using a commercial kit (Sigma-Aldrich) according to the manufacturer's instructions (Lin et al., 2019).

2.14. Bio-distribution study

All animal studies were approved, maintained, treated, housed and performed in accordance with the guideline of institutional animal ethical committee (Registration no. 883/PO/ReBi/S/05/CPCSEA and project no. IP/PCEU/PHD/24/2018/013).

In-vivo biodistribution of pure LT, LT-PLGA NPs and Chitosan@LT-PLGA C/SNPs was performed in male Sprague Dawley (SD) rats (weight range 250–350 g). Male Sprague Dawley (SD) rats with a weight ranging from 250 to 350 g were selected for in-vivo biodistribution study. SD rats were divided into 4 groups each consisting of 6 animals. Group I animals were administered with LT suspension and group II received the LT-PLGA NPs and group III received Chitosan@LT-PLGA C/SNPs (fluorescently labelled) equivalent to 4 mg/kg of LT, respectively and group IV was considered as control. The method for biodistribution was followed which was previously reported with some modifications (Navarro et al., 2014). The tissues of control group were utilized for calibration curve when they were sacrificed. The standard curves were plotted distinctly for each tissues i.e. liver, kidney, lungs, brain, heart and spleen.

The 50 µl of formulation was instilled in each nostril of rats. Rats were held from the back in slanted position during intranasal administration. Animals were sacrificed and different organs were isolated after predetermined time points (i.e. 12 and 24 h). The organs were homogenized using a tissue homogenizer with 5 ml of PBS and the homogenate was centrifuged at 15000 rpm for 30 min. the supernatant was collected and filtered through 0.45 µm filter and analysed using spectroflurometer (Pandey et al., 2019).

2.15. In-vivo pharmacokinetic study

All animal studies were approved, maintained, treated, housed and performed in accordance with the guideline of institutional animal ethical committee (Registration no. 883/PO/ReBi/S/05/CPCSEA and project no. IP/PCEU/PHD/24/2018/013).

Pharmacokinetic of pure LT, LT-PLGA NPs and Chitosan@LT-PLGA C/SNPs was performed in male Sprague Dawley (SD). Rats with a weight ranging from 250 to 350 g were selected for in-vivo pharmacokinetic study. SD rats were divided into 6 groups each consisting of 6 rats. Group I and II animals were administered with LT suspension intranasally and intravenously, respectively; group III received the LT-PLGA NPs (intranasal), group IV received LT-PLGA NPs (intravenous), group V received Chitosan@LT-PLGA C/SNPs (intranasal) and group VI received Chitosan@LT-PLGA C/SNPs (intravenous) equivalent to 4 mg/kg of LT, respectively. For group I, II and IV, the 50 µl of formulation was instilled in each nostril of rats using micropipette attached with LDPE tubing, having internal diameter of 0.1 mm at the delivery site. Rats were held from the back in slanted position during intranasal administration. To group III and V, 50 µl of formulation was injected intravenously through the tail. After predetermine time 0.5, 1, 2, 4, 12 h point after the administration of samples, 0.5 ml of blood from *retro*-orbital plexus of rats was collected into heparinized tubes. The plasma and brain were separated and was stored at −70 °C until HPLC analysis (Shimadzu (Shimadzu Corporation, Kyoto, Japan)) (Karlina et al., 2008). Acetonitrile was added to brain homogenate and vortexed for 5 min and then centrifuged for 15 min at 10,000 rpm at 8 °C to remove precipitated proteins. For HPLC analysis, acetonitrile: methanol (95:5 v/v) was used as mobile phase and flow rate of 1 ml/min. sample volume with 20 µl was injected in HPLC column (Kromasil C-18 (particle size 5 µm, 4.6 mm × 250 mm), Amsterdam, Netherland) and analysed. The LT detection wavelength was 450 nm. The pharmacokinetic parameters were calculated using kinetica 5.0 software. The graph was plotted with LT concentration (brain and plasma) against time. The drug targeting efficiency (DTE%) and direct transport percentage (DTP %) was calculated using following formula

$$DTE\% = [(AUC_{brain}/AUC_{blood})_{i,n}/(AUC_{brain}/AUC_{blood})_{i,v}] * 100$$

$$DTP\% = (B_{i.n} - -B_x/B_{i.n}) * 100$$

Where,

AUC is area under curve;

$B_x = (B_{i.v}/P_{i.v}) * P_{i.n}$ (B_x is the brain AUC fraction contributed by systemic circulation through the BBB following intranasal administration);

$P_{i.v}$ is the $AUC_{0\text{-}12h}$ (blood) following intravenous administration;

$P_{i.n}$ is the $AUC_{0\text{-}12h}$ (blood) following intranasal administration

$B_{i.n}$ is the $AUC_{0\text{-}12h}$ (brain) following intranasal administration

$B_{i.v}$ is the $AUC_{0\text{-}12h}$ (brain) following intravenous administration

2.16. In-vivo toxicity studies

The systemic toxicity study was approved by the Institutional Animal Ethical Committee, Institute of Pharmacy, Nirma University. The systemic toxicity of formulated NPs was assessed in mice and study was planned according to standard guidelines (Pandey et al., 2020). The study involved 3 groups containing 6 mice/group. Group 1 (control)- Milli-Q water; Group 2: LT-PLGA NPs; Group 3: Chitosan@LT-PLGA C/SNPs. Equivalent amount of LT-PLGA NPs and Chitosan@LT-PLGA C/SNPs (containing 4 mg LT/kg of body weight of mice) (0.5 ml) was daily administered intranasally for seven consecutive days. Further,

blood samples were collected for biochemical analysis by cardiac puncture and then animals were sacrificed humanely by administering sodium pentobarbital (60 mg/kg) intravenously. The liver was excised from all three groups, washed in ice cold PBS to remove superficial blood and stored at −80 °C for further study. Several haematological and biochemical parameters were measured to assess toxicity caused due to LT-PLGA NPs and Chitosan@LT-PLGA C/SNPs.

2.17. Stability studies

2.17.1. Photo-stability study

The ability of NPs to protect LT from photo-degradation was performed by exposing LT suspension, LT-PLGA NPs and Chitosan@LT-PLGA C/SNPs to UV light to UV-C 260 nm TUV T5 lamp (Philips, India) for 24 h (Ranganathan et al., 2019). Briefly, known quantity of LT and equivalent weight of LT-PLGA NPs and Chitosan@LT-PLGA C/SNPs were dispersed in phosphate buffer (pH 7.4) containing 0.5% tween 80 and kept in different glass vials. Aliquots were collected at fixed time interval of 4 h. Ethanolic solution of BHT (0.1% w/v) was added in the collected aliquots to avoid oxidation. The samples were further treated with nitrogen and covered with aluminium foil for prevention of further oxidative losses (Ranganathan et al., 2019). Later, LT was extracted and quantified using spectrofluorometer. The LT stability was measured using following equation

$$stabilityofLT\,(\%) = \frac{Ct}{C0} * 100 \quad (4)$$

Where, C_t and C_0 indicates LT concentration at t time and initial time

2.17.2. Thermal stability study

Lyophilized powder of LT-PLGA NPs and Chitosan@LT-PLGA C/SNPs and pure LT was redispersed in deionized water (1 mg/ml). The formed colloidal solutions were filled in amber colour vials and exposed at 4 °C, 25 °C and 30 °C for 30 days. The samples were tested at 0, 7, 15 and 30 day (time interval) for particle size, PDI and surface charge (Chittasupho et al., 2018).

2.18. Statistical analysis

All the results were analysed using the statistical software package Graph Pad Prism. All the experiments were performed thrice and were expressed as mean ± SD. The experimental data was validated by one-way ANOVA for statistical significance, wherever applicable.

3. Result and discussion

3.1. Fabrication and optimization of NPs (core NPs and C/SNPs)

The placebo PLGA NPs and LT-PLGA NPs were fabricated using nanoprecipitation method. The optimization was done by varying several factors viz. LT concentration, PLGA concentration, organic to aqueous phase ratio, surfactant concentration, stirring speed, stirring time and addition rate (data not shown). The optimized values of independent variables for the preparation of LT-PLGA NPs are shown in Table 1.

Placebo Chitosan@PLGA C/SNPs and Chitosan@LT-PLGA C/SNPs were fabricated by functionalizing chitosan over the surface of PLGA NPs via electrostatic interactions for improving cellular uptake and brain bioavailability of LT. The coating of shell was performed by varying chitosan concentration and stirring time and was optimized through particle size and zeta potential of Chitosan@PLGA C/SNPs as depicted in Fig. 1A. The results demonstrated that chitosan concentration and stirring time have positive effect on particle size of Chitosan@PLGA C/SNPs. As the chitosan concentration increased the particle size of Chitosan@PLGA C/SNPs increased, and it may be due to maximum amount of chitosan deposited on PLGA NPs. Similarly, as the stirring time increased the particle size also increased, it may be due to the fact that as time lapse the more amount of chitosan can be deposited on PLGA NPs resulting into large thickness of shell. Chitosan concentration and stirring time showed significant effect on PDI after specific chitosan concentration and stirring time for example, with 0.02% w/v and 0.03% w/v of chitosan concentration, PDI did not showed significant effect till 45 min, however, at 60 min, the colloidal solution of Chitosan@PLGA C/SNPs showed polydispersivity with PDI greater than 1. In addition, at chitosan concentration of 0.04% w/v after 30 min, the colloidal solution of Chitosan@PLGA C/SNPs exhibited polydispersivity. The results obtained may be due to interlinking of chitosan molecules within each other and with PLGA, resulting into un-uniform size distribution of colloidal solution. Similarly, both chitosan concentration and stirring time showed significant positive effect on zeta potential of Chitosan@PLGA C/SNPs. The results demonstrated that as chitosan concentration and stirring time increased, the zeta potential of Chitosan@PLGA C/SNPs was increased towards positive. From above obtained results, 0.01% w/v of chitosan concentration with 15 min of stirring time was selected as optimized values to achieve lower increment in size and PDI.

Table 1
Optimized values of independent variables for the preparation of LT-PLGA NPs.

Parameters	values
PLGA concentration	5 mg/ml
Surfactant concentration	1% w/v
Lutein concentration	2 mg
Organic : aqueous ratio	1: 6
Stirring speed	500 rpm
Addition rate	1 ml/min

The lyophilisation of placebo PLGA NPs, placebo Chitosan@PLGA C/S NPs, LT-PLGA NPs and Chitosan@LT-PLGA C/S NPs was performed using mannitol as a cryoprotectent with the concentration of 5%, as the lower concentration (1%) and higher concentration (10%) of cryoprotectent leads to aggregation of NPs resulting into increase in particle size with non-uniform distribution of the particles. The results indicated that there was no significant change in the particle size, PDI and zeta potential between the samples before and after lyophilisation. The obtained results may be owing to the presence of cryoprotectent used in the process of lyophilisation. Aldawsari et al. very well explained the effect of cryoprotectent concentration on particle size, PDI and zeta potential. The results indicated that 5% of trehalose was the optimized concentration for lyophilisation to obtained insignificant change in particle size, PDI and zeta potential. The study revealed that 1% of cryoprotectent may lead to the increase in particle size; however, as the concentration increases to 5%, the particle size of NPs decreases significantly. Additionally, as the cryoprotectent concentration increases to 10%, there was no significant change in particle size with respect to 5%. The similar pattern was obtained for PDI too. Moreover, the increase in cryoprotectent concentration showed insignificant effect on zeta potential (Aldawsari et al., 2020).

3.2. Characterization of NPs (core NPs and C/SNPs)

The mean particle size, PDI and zeta potential of placebo PLGA NPs and LT-PLGA NPs was found to be 128.8 ± 1.25 nm and 136.2 ± 1.09 nm; 0.096 ± 0.007 and 0.093 ± 0.005; −38.10 ± 1.03 mV and −27.29 ± 0.97 mV, respectively. As compared to placebo PLGA NPs, the size of LT-PLGA NPs was increased which may due to encapsulation of LT within the PLGA NPs. The increase in the LT concentration resulted into greater particle size and PDI, thus lutein concentration has positive impact on particle size and PDI. The lower value of PDI of optimized formulation indicated

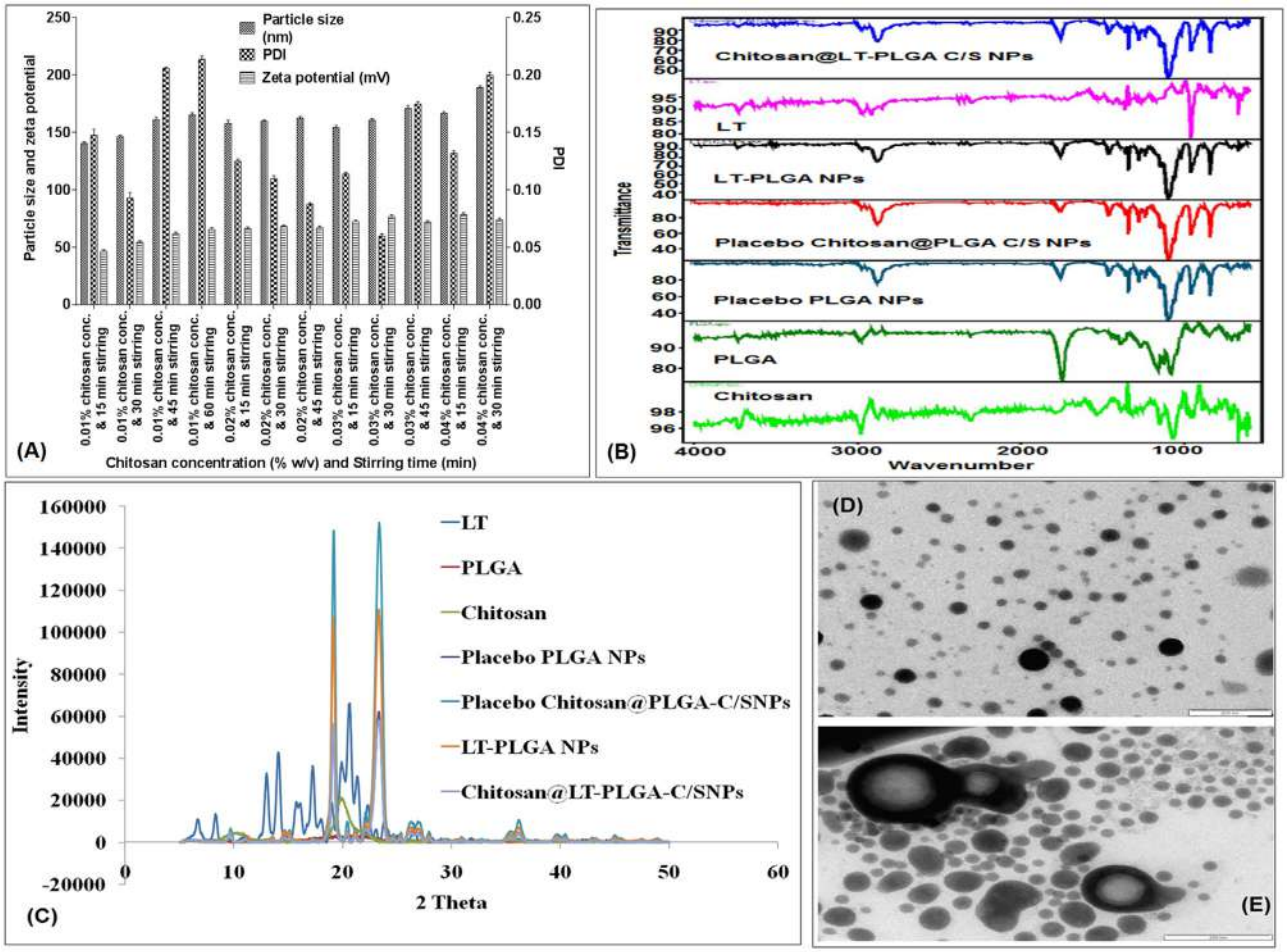

Fig. 1. Optimization of chitosan coating over PLGA NPs (A); Characterization of pure LT, LT-PLGA NPs and Chitosan@LT-PLGA C/SNPs by FTIR (B);pXRD (C); and TEM of LT-PLGA NPs(D); TEM of Chitosan@LT-PLGA C/SNPs (E).

uniformity of particle distribution. The negative surface charge on PLGA NPs is owing to ionized carboxyl group in PLGA (Dhas et al., 2015). More negativity of surface charge indicates its stability.

The mean particle size, PDI and zeta potential of placebo Chitosan@PLGA C/SNPs and Chitosan@LT-PLGA C/SNPs was found to be 134.6 ± 2.01 nm and 142.3 ± 2.57 nm; 0.090 ± 0.03 and 0.091 ± 0.09; + 54.8 ± 2.15 mV and + 46.6 ± 1.87 mV, respectively. The results revealed that as compared to placebo PLGA NPs and LT-PLGA NPs, the particle size of placebo Chitosan@PLGA C/SNPs and Chitosan@LT-PLGA C/SNPs was found to be higher indicating that chitosan is coated over the PLGA NPs (Dhas et al., 2015). It was further confirmed by TEM analysis. The positive charge on surface of Chitosan@PLGA C/SNPs is owing to chitosan and it also indicates chitosan is well coated over PLGA NPs to form Chitosan@PLGA C/SNPs. More positive charge over the Chitosan@PLGA C/SNPs surface indicates its stability.

The amount LT entrapped in the LT-PLGA NPs and Chitosan@LT-PLGA C/SNPs was determined using sephadex column. The LT-PLGA NPs and Chitosan@LT-PLGA C/SNPs were successfully passed through the sephadex column whereas the un-entrapped LT was blocked in the column which was collected by passing LT soluble solvent. LT was estimated in UV-spectrophotometer at λmax of 446 nm. The results indicated that the %EE in optimized LT-PLGA NPs and Chitosan@LT-PLGA C/SNPs was found to be 84.35% ± 1.69%, 83.97 ± 1.03%, respectively while %DL was found to be 4.61% ± 0.05%, 3.95 ± 0.03%, respectively.

The FTIR spectrums of pure LT, PLGA, chitosan, placebo PLGA NPs, placebo Chitosan@PLGA C/SNPs, LT-PLGA NPs and Chitosan@LT-PLGA C/SNPs were shown in Fig. 1B. Pure LT displayed characteristic peaks at 3420.19 cm^{-1} indicating presence of free O–H; 2916.37 cm^{-1} and 2970.38 cm^{-1} peaks indicates presence of C–H aldehyde; 1039.63 cm^{-1} peak indicates the presence of secondary –OH group (Ranganathan et al., 2019). The characteristic peak of pure chitosan at 1070.49 cm^{-1} is owing to C = O group stretching; 1517.98 cm^{-1} is assigned to the presence of stretching of free amino group; 1668.43 cm^{-1} is relative to the vibration of the carbonyl group of acetylated amide; 3469.72 cm^{-1} indicates that the O–H stretching overlapped with and N–H stretching vibration (Tzeyung et al., 2019). The PLGA showed characteristic peaks at 1082 cm^{-1} for C-O-C stretching, 1752 cm^{-1} for C = O stretching as well as 2972.31 cm^{-1} for C–H group (Lu et al., 2019). In case of placebo PLGA NPs, all the characteristic peaks of PLGA were present. Placebo Chitosan@PLGA C/SNPs showed characteristic peaks of chitosan and PLGA indicating chitosan was coated over PLGA, also did not displayed any additional peak which indicates compatibility of both the polymers. Furthermore, in case of LT-PLGA NPs and Chitosan@LT-PLGA C/SNPs, the characteristic peaks of LT were absent indicating that LT might be encapsulated in PLGA NPs and Chitosan@PLGA C/SNPs (Ranganathan et al., 2019)

XRD patterns of all samples viz. pure LT, chitosan, PLGA, placebo PLGA NPs, placebo Chitosan@PLGA C/SNPs, LT-PLGA NPs and Chitosan@LT-PLGA C/SNPs were carried out to study the crystalline nature and depicted in Fig. 1C. The diffractogram of pure LT exhibited intense peaks at 2θ values of 14.06 and 20.64, indicating the crystallinity of LT (Muhoza et al., 2018), whereas diffractogram of chitosan showed intense peak at 2θ values of 19.82, revealing high degree of

crystallinity (Tzeyung et al., 2019). However, PLGA did not show any sharp intense peak indicating its amorphous nature (Deepika et al., 2019). The diffractograms of lyophilized powder of placebo PLGA NPs, placebo Chitosan@PLGA C/SNPs, LT-PLGA NPs and Chitosan@LT-PLGA C/SNPs demonstrated diminished characteristic peaks of LT as compared to pure LT, which revealed that crystalline nature of LT has decreased and has been dispersed molecularly in the PLGA matrix. However, the intense peak at 2θ values of 19.18 and 23.34, in lyophilized placebo PLGA NPs, placebo Chitosan@PLGA C/SNPs, LT-PLGA NPs and Chitosan@LT-PLGA C/SNPs were the characteristic peaks of mannitol (Mathur et al., 2019).

The morphological TEM images demonstrate that LT-PLGA NPs and Chitosan@LT-PLGA C/SNPs both were spherical with smooth surface and uniform size distribution in the range of 110–150 nm, which are depicted in Fig. 1D and 1E. The spherical and smooth surface of NPs has great importance as it leads to less adsorption of plasma protein and further opsonisation and therefore is poor substrates of liver and RES uptake. However, the chitosan was uniformly coated over the PLGA NPs forming Chitosan@LT-PLGA C/SNPs as indicated in Fig. 1E. The resulting size of LT-PLGA NPs and Chitosan@LT-PLGA C/SNPs obtained from TEM resembles the data of particle size obtained by particle size analyser.

3.3. In-vitro release study

One of the objectives of study was to explore the effect of chitosan coating (shell) on LT release behaviour from PLGA NPs. In-vitro release of LT from LT suspension, LT-PLGA NPs and Chitosan@LT-PLGA C/SNPs is depicted in Fig. 2A. The results showed that LT suspension released almost 52.6 ± 1.4% of LT from its suspension form after 6 h and 76.9% of LT after 24 h, indicating sustained release was not obtained, whereas, LT release from LT-PLGA NPs showed biphasic release behaviour i.e with initial burst release was found to be 25.71 ± 1.35% upto 6 h and followed by slow and sustained release i.e. after 96 h, 87.27 ± 1.36% of LT release from PLGA NPs was observed. The biodegradable polymers usually follow three distinct mechanisms for drug release i.e. desorption of drug from NP's surface, diffusion from the polymer matrix followed by re-adsorption, degradation, dissolution/erosion of the polymeric network. The burst release of LT may be due to adsorption of LT on PLGA NPs's surface along with more solubility of LT in dissolution media (Ahmad et al., 2020). Similarly, LT release from Chitosan@LT-PLGA C/SNPs also showed slow but steady release at each time point as compared to LT-PLGA NPs. It was found that after 6 h, the LT release from Chitosan@LT-PLGA C/SNPs was found to be 17.64 ± 1.27%, followed by more sustained release i.e. only 70.12 ± 1.25% of LT was released after 96 h. owing to the presence of chitosan coating (shell) there was no burst release observed which indicates that chitosan coating act as physical barrier for PLGA NPs limiting its diffusion/erosion process of LT from PLGA NPs (Khan et al., 2018).

3.4. Ex-vivo diffusion study

Ex-vivo diffusion study was conducted on goat nasal mucosa using Franz-diffusion cell for 24 h. The results demonstrated that LT from Chitosan@LT-PLGA C/SNPs was more permeated through nasal mucosal membrane as compared to LT from LT-PLGA NPs and pure LT suspension and are depicted in Fig. 2B. The results demonstrated that LT from LT suspension was permeated up to 47.6% after 24 h. However, LT from LT-PLGA NPs and Chitosan@LT-PLGA C/SNPs exhibited 71.73% and 87.01% of release after 24 h. The higher permeation of LT from Chitosan@LT-PLGA C/SNPs through nasal mucosa was owing to the presence of cationic chitosan over the surface of PLGA NPs which act as a permeation enhancer (Ahmad et al., 2020). Cationic group of chitosan interacted with anionic group of nasal membrane is also involved in permeation enhancement of Chitosan@LT-PLGA C/SNPs (Khan et al., 2018). Apart from this chitosan also has the ability to open tight junctions of nasal mucosa.

3.5. Cellular uptake of prepared NPs

Quantitative cellular internalization of prepared NPs viz. FITC conjugated placebo PLGA NPs, FITC conjugated placebo Chitosan@PLGA C/SNPs, FITC conjugated LT-PLGA NPs and FITC conjugated Chitosan@LT-PLGA C/SNPs and FITC (as control) using SH-SY-5Y cell line was performed and evaluated by spectrofluorometer. The results (Fig. 3A) revealed that fluorescence intensity of FITC conjugated NPs was much higher inside the cell than that of control group (FITC). However, Chitosan@LT-PLGA C/SNPs exhibited higher fluorescence intensity as compared to other NPs. The results demonstrated that FITC showed 1.7% of cellular uptake whereas placebo PLGA NPs, placebo Chitosan@PLGA C/SNPs, LT-PLGA NPs and Chitosan@LT-PLGA C/SNPs showed 39.6 ± 3.9%, 38.1 ± 4.1%, 40.3 ± 4.4% and 51.6 ± 5.2% of cellular uptake, respectively. The above results revealed that surface modification can influence the cellular internalization of NPs. The previous investigations demonstrated that cationic NPs are easily attracted towards endothelial cells owing to electrostatic interactions between cationic NPs and anionic cell membranes as compared to negatively charged and neutral surface of NPs (Cho et al., 2009). Secondly owing to the coating of chitosan, Chitosan@PLGA C/SNPs have more hydrophilic surface which leads to greater cellular internalization (Sahoo et al., 2002). Thus, study demonstrated that owing to the chitosan shell over PLGA NPs, the cellular internalization of LT enhanced also le to rapid absorption when administered intranasally.

Similar results were obtained from qualitative cellular internalization analysis. The results demonstrated that fluorescence intensity of Chitosan@LT-PLGA C/SNPs (Fig. 3C) in cells was higher than that of LT-PLGA NPs (Fig. 3B) indicating higher internalization of C/SNPs in the cells.

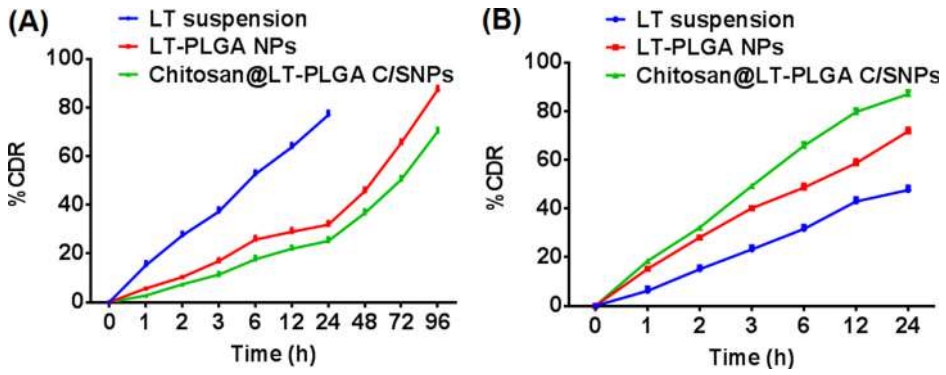

Fig. 2. *In-vitro* release study (A) and *Ex-vivo* permeation study (B) of pure LT,LT-PLGA NPs and Chitosan@LT-PLGA C/SNPs.

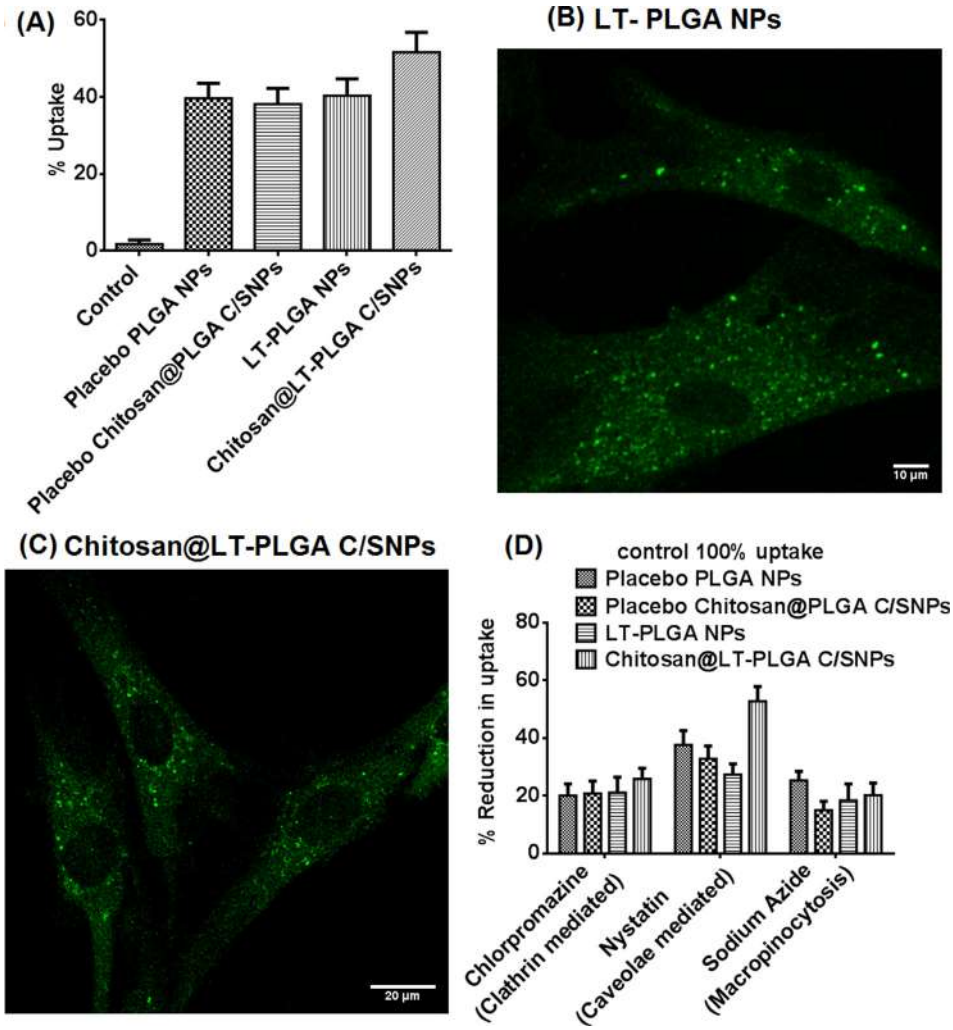

Fig. 3. Quantitative cellular uptakeof LT-PLGA NPs and Chitosan@LT-PLGA C/SNPs (A); Qualitative cellular uptake of LT-PLGA NPs (B); Qualitative cellular uptake of Chitosan@LT-PLGA C/SNPs(C); Cellular internalization mechanism of placebo PLGA NPs, placebo Chitosan@PLGA C/SNPs, LT-PLGA NPs and Chitosan@LT-PLGA C/SNPs (D).

3.6. Cellular uptake mechanism study

Cellular internalization mechanisms of prepared NPs were elucidated using various endocytic pathway inhibitors such as chlorpromazine (clathrin-mediated), nystatin (caveolae-mediated) and sodium azide (macropinocytosis) using SH-SY-5Y cell line and analysed by spectrofluorometer and results are depicted in Fig. 3D. The results revealed that when chlorpromazine was exposed to SH-SY-5Y cells, the cellular internalization of placebo PLGA NPs, placebo Chitosan@PLGA C/SNPs, LT-PLGA NPs and Chitosan@LT-PLGA C/SNPs was reduced to 19.95 ± 4.10%, 20.73 ± 4.30%, 21.09 ± 5.30% and 25.78 ± 3.70%, respectively (% reduction in internalization). The above results demonstrated that clathrin-mediated pathway was one of the pathways for the internalization of NPs. In general, clathrin-mediated pathway involves in selective uptake of molecules through specific receptors. Several investigations have reported that NPs with particle size less than 200 nm follows the clathrin-mediated pathway for cellular internalization (Hillaireau and Couvreur, 2009). When sodium azide was exposed to SH-SY-5Y cells, the cellular internalization of placebo PLGA NPs, placebo Chitosan@PLGA C/SNPs, LT-PLGA NPs and Chitosan@LT-PLGA C/SNPs was reduced to 25.25 ± 3.20%, 14.96 ± 3.10%, 18.36 ± 5.70% and 20.16 ± 4.20%, respectively. The results demonstrated that macropinocytosis pathway was also one of the pathways for the internalization of NPs, nevertheless at very lesser extent. Macropinocytosis involves in formation of actin, where NPs with particle size around 200 nm can be internalize into cells through the formation of vesicles of around 0.2 to 5 µm (Conner and Schmid, 2003; Mukherjee et al., 1997). Further, positive charge on the surface or hydrophilic nature of C/SNPs might help in the formulations to escape the uptake through macropinocytosis and thus avoiding the lysosomal degradation. Lysosome plays significant role in therapeutic fate of NPs applicable for neurodegenerative diseases such as AD, since the NPs following macropinocytosis would be vulnerable to degradation (Paka and Ramassamy, 2017). The results suggested that clathrin-mediated pathway was more followed by NPs as compared to macropinocytosis pathway for cellular internalization. Further, when nystatin was exposed to SH-SY-5Y cells, the cellular internalization of placebo PLGA NPs, placebo Chitosan@PLGA C/SNPs, LT-PLGA NPs and Chitosan@LT-PLGA C/SNPs was significantly reduced to 37.63 ± 4.90%, 32.81 ± 4.40%, 27.30 ± 3.70% and 52.71 ± 5.10%, respectively. The results demonstrated that amongst all three pathways, the internalization of prepared NPs were much higher by caveolae-mediated endocytosis-based pathway as compared to clathrin-mediated pathway and macropinocytosis. The results can be further explained in the way that caveolae are most abundantly found on endothelial cells, where they can constitute 10–20% at the cell surface (Conner and Schmid, 2003; Rejman et al., 2004).

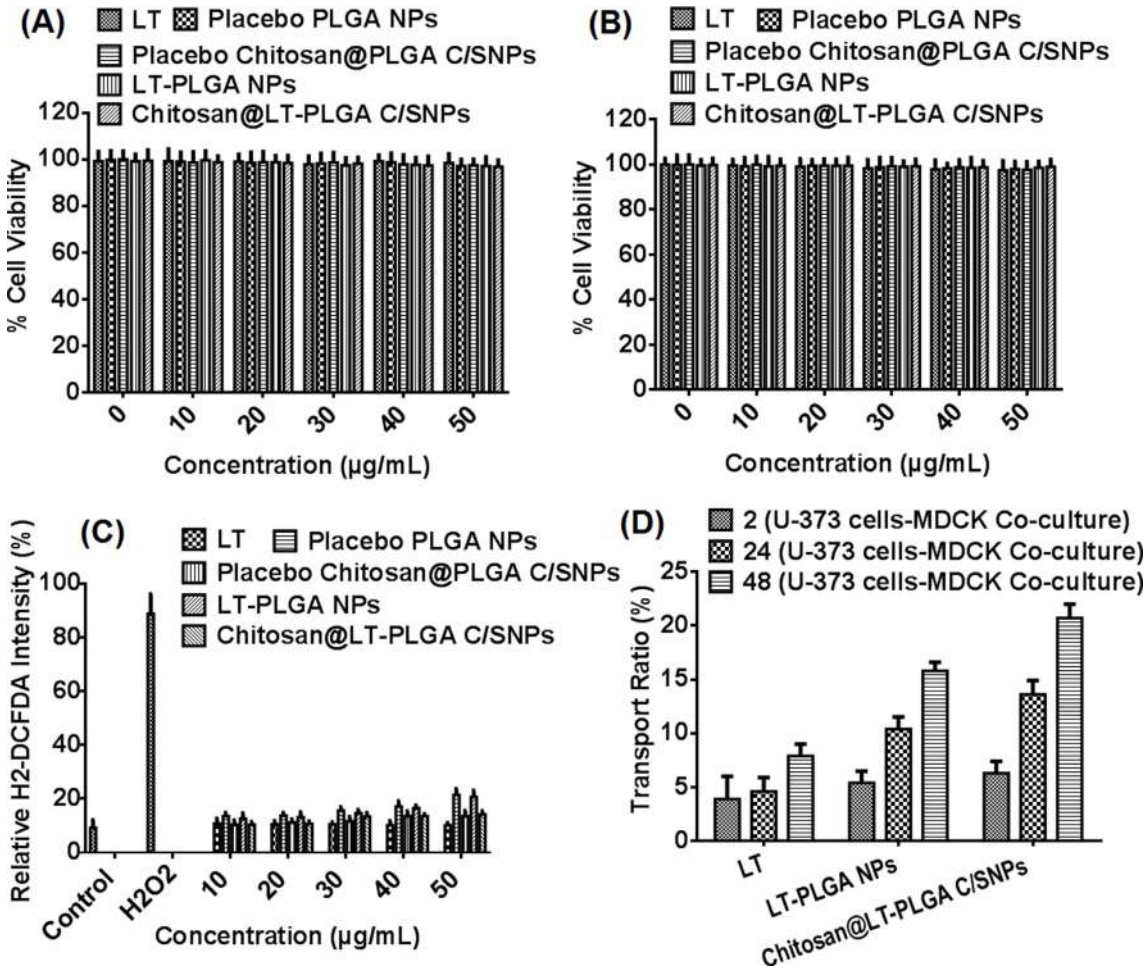

Fig. 4. Elucidation of *in-vitro* cell line studies of pure LT, placebo PLGA NPs, placebo Chitosan@PLGA C/SNPs, LT-PLGA NPs and Chitosan@LT-PLGA C/SNPs: MTT assay on SH-SY-5Y cell line (A) and RPMI 2650 cell line (B); ROS generation on RAW 264.7 cell line (C); BBB permeation study using co-culture model (MDCK II and U 373 MG cells) (D).

3.7. In-vitro cell viability assay

The cell viability assay was conducted on two cell lines i.e. SH-SY-5Y (Fig. 4A) and RPMI 2650 (Fig. 4B) cell line, to study the biocompatibility and safety of formulated NPs. The results indicated that when the cells were exposed to different concentrations (0, 10, 20, 30 40 50 µg/ml) of pure LT, placebo PLGA NPs, placebo Chitosan@PLGA C/SNPs, LT-PLGA NPs and Chitosan@LT-PLGA C/SNPs for 24 h, there were no reduction in the cell viability was observed in both the cell lines. The % cell viability of all the samples was found to be greater than 90% after 24 h of exposure. As chitosan and PLGA has been approved by FDA as GRAS category and lutein being beta-carotenoid, we can suggest that developed nanoparticles are biocompatible and do not cause cell cytotoxicity till 50 µg/ml of concentration. From the investigation it can be concluded that all the samples, pure LT, placebo PLGA NPs, placebo Chitosan@PLGA C/SNPs, LT-PLGA NPs and Chitosan@LT-PLGA C/SNPs were found to be safe in both SH-SY-5Y and RPMI 2650 cell lines. Since these formulations are formulated for intranasal administration and nasal epithelium (RPMI-2650 cell line) represents first barrier and neuronal cells (SH-SY-5Y cell line) represents second exposure site for NPs, the results indicated their biocompatibility and safety, independently of surface charge.

3.8. ROS generation study

The ROS generation study for all prepared NPs was performed using RAW 264.7 cell line. Various samples viz. pure LT, placebo PLGA NPs, placebo Chitosan@PLGA C/SNPs, LT-PLGA NPs and Chitosan@LT-PLGA C/SNPs at different concentrations (10, 20, 30, 40 and 50 µg/ml) were exposed to RAW 264.7 cells, whereas control group indicates the cells with no treatment of formulations/NPs. The results (Fig. 4C) demonstrated that control group exhibited the relative fluorescent intensity of 9.2 ± 2.9%. Likewise, when different concentrations of pure LT, placebo PLGA NPs, placebo Chitosan@PLGA C/SNPs, LT-PLGA NPs and Chitosan@LT-PLGA C/SNPs were exposed to RAW 264.7 cells, they exhibited insignificant change in the relative fluorescent intensity in the cells. Briefly, pure LT, placebo PLGA NPs, placebo Chitosan@PLGA C/SNPs, LT-PLGA NPs and Chitosan@LT-PLGA C/SNPs at a concentration of 50 µg/ml exhibited relative fluorescent intensity of 10.2 ± 0.9%, 21.4 ± 2.3%, 13.5 ± 2.1%, 20.7 ± 2.4% and 14.2 ± 1.3%, respectively, which is insignificant when compared to control. On the contrary, when H2O2 was exposed to RAW 264.7 cells exhibited significant increase in relative fluorescent intensity in the cells suggesting greater ROS generation into the cell was obtained, i.e. 88.7 ± 7.4%, which was far greater than that of relative fluorescent intensity obtained in the cells treated with formulations and control group. Thus, in a conclusion, the ROS generation investigation revealed that pure LT, placebo PLGA NPs, placebo Chitosan@PLGA C/SNPs, LT-PLGA NPs and Chitosan@LT-PLGA C/SNPs, till the concentration of 50 µg/ml was not generating ROS, suggesting that till this concentration, these formulations are safe, as increase in ROS generation leads to decrease in cell viability. Therefore, aforementioned concentration of LT-PLGA NPs and

Chitosan@LT-PLGA C/SNPs can be employed in AD for antioxidant activity.

3.9. In-vitro BBB permeation study

In this study co-culture of U 373 MG cells and MDCK II cells was utilized as in-vitro BBB model. The results revealed that transport ratio of LT-PLGA NPs and Chitosan@LT-PLGA C/SNPs were higher as compared to pure LT as depicted in Fig. 4D. In addition, the results also showed that internalization of NPs was time dependent. In brief, after exposure of NPs for 2 h, the transport ratio of pure LT, LT-PLGA NPs and Chitosan@LT-PLGA C/SNPs through in-vitro co-culture model of BBB was found to be 3.9 ± 2.1%, 5.4 ± 1.1% and 6.3 ± 1.1%, respectively. However, after 25 h, the transport ratio of pure LT, LT-PLGA NPs and Chitosan@LT-PLGA C/SNPs through in-vitro co-culture model of BBB was found to be 4.6 ± 1.3%, 10.4 ± 1.1% and 13.6 ± 1.3%, respectively. Whereas, after 48 h, the transport ratio of pure LT, LT-PLGA NPs and Chitosan@LT-PLGA C/SNPs through in-vitro co-culture model of BBB was found to be 7.9 ± 1.1%, 15.8 ± 0.8% and 20.7 ± 1.3%, respectively. Therefore, from in to vitro BBB permeation study it can said that LT when loaded in NPs more specifically C/SNPs exhibited more permeation as compared to pure LT. Thus, the amount NPs which entered the blood circulation from nasal cavity, can effectively cross the BBB and exhibit its activity at site of action.

3.10. Antioxidant assay

The antioxidant activity of prepared NPs was determined using three distinct assays viz. SOD, CAT and MDA. It was characterized by activity of antioxidant enzymes in pure LT, LT-PLGA NPs and Chitosan@LT-PLGA C/SNPs-treated cells under oxidative stress. The results (Fig. 5A) demonstrated that as compared to positive control group, the lower concentration (5 mM and 10 mM) of pure LT showed significant increase in SOD activity when cells were exposed to H_2O_2 for 8 h. However, at higher concentration (20 mM) of pure LT showed significant reduction in SOD activity as compared to negative control group. Similarly, as compared to positive control group, at lower concentration (5 mM) of LT-PLGA NPs and Chitosan@LT-PLGA C/SNPs showed significant increase in SOD activity when cells were exposed to H_2O_2 for 8 h. However, at higher concentration (10 mM and 20 mM) of LT-PLGA NPs and Chitosan@LT-PLGA C/SNPs led to significant reduction in SOD activity as compared to negative control group. SOD catalyzes the O_2– (superoxide) radical to form either H_2O_2 or ordinary molecular oxygen (O_2). In the similar manner, all the concentrations of pure LT, LT-PLGA NPs and Chitosan@LT-PLGA C/SNPs have demonstrated significant increase in CAT activity as compared to both the controls i.e. positive and negative control (Fig. 5B). The MDA assay indicated that after 8 h of exposure of various concentrations of pure LT, LT-PLGA NPs and Chitosan@LT-PLGA C/SNPs have significantly lower MDA level as compared to positive control group. Additionally, the MDA level was significantly increased in the positive control group as compared to negative control group (Fig. 5C) (Daverey and Agrawal, 2018; Lin et al., 2019). The overall results demonstrated that lower concentration of pure LT, LT-PLGA NPs and Chitosan@LT-PLGA C/SNPs exhibited significant effect on ROS scavenging. However, higher dose of pure LT, LT-PLGA NPs and Chitosan@LT-PLGA C/SNPs can induce the ROS generation.

3.11. Biodistribution study

The biodistribution of FITC conjugated LT-PLGA NPs and FITC conjugated Chitosan@LT-PLGA C/SNPs were measured using obtained calibration curve in various organs. The results of biodistribution study were expressed as percentage dose per gram of tissue (% total dose/g) to compensate for possible variation between animals and are depicted in Fig. 6. The results indicated that the amount of LT in various organs such as liver, kidney, lungs, brain, heart and spleen was found to be 0.12 ± 0.05%, 0.21 ± 0.04%, 0.24 ± 0.03%, 0.09 ± 0.02%, 0.13 ± 0.03% and 0.42 ± 0.07%, respectively after 12 h of intranasal administration. Whereas, after 24 h of intranasal administration, the amount of LT in liver, kidney, lungs, brain, heart and spleen was found to be 0.17 ± 0.03%, 0.31 ± 0.03%, 0.25 ± 0.08%, 0.15 ± 0.04%, 0.17 ± 0.03%, 0.55 ± 0.12%, respectively. However, the amount of FITC conjugated LT-PLGA NPs in various organs like liver, kidney, lungs, brain, heart and spleen was found to be 0.15 ± 0.04%, 0.13 ± 0.05%, 0.16 ± 0.03%, 0.17 ± 0.03%, 0.17 ± 0.05% and 0.39 ± 0.02%, respectively after 12 h of intranasal administration. Whereas, after 24 h of intranasal administration, the amount of FITC conjugated LT-PLGA NPs in various organs viz. liver, kidney, lungs, brain, heart and spleen was found to be 0.19 ± 0.04%, 0.25 ± 0.04%, 0.21 ± 0.05%, 0.28 ± 0.07%, 0.19 ± 0.03% and 0.48 ± 0.08%, respectively. Additionally, the amount of FITC conjugated Chitosan@LT-PLGA C/SNPs in various organs like liver, kidney, lungs, brain, heart and spleen was found to be 0.17 ± 0.02%, 0.13 ± 0.03%, 0.14 ± 0.02%, 0.29 ± 0.05%, 0.14 ± 0.04% and 0.53 ± 0.07%, respectively after 12 h of intranasal administration. Whereas, after 24 h of intranasal administration, the amount of FITC conjugated Chitosan@LT-PLGA C/SNPs in various organs viz. liver, kidney, lungs, brain, heart and spleen was found to be 0.19 ± 0.04%, 0.24 ± 0.05%, 0.22 ± 0.03%, 0.49 ± 0.11%, 0.25 ± 0.06% and 0.55 ± 0.09%, respectively. The results suggested that after 24 h of intranasal administration, the biodistribution of FITC-LT-PLGA NPs and FITC-Chitosan@LT-PLGA C/SNPs was higher in each organ as compared to 12 h. However, as compared to LT-PLGA NPs, the amount of Chitosan@LT-PLGA C/SNPs was found higher in brain, indicating that chitosan-based surface modification of PLGA NPs can enhance targeting efficiency to the brain. Additionally, highest amount of LT, FITC-LT-PLGA NPs and FITC- Chitosan@LT-PLGA C/SNPs in spleen can be explained by fact that when LT, FITC-LT-PLGA NPs and FITC-Chitosan@LT-PLGA C/SNPs entered the systemic circulation interacts with coagulation factors, blood cells and plasma proteins and these interacted product recognized by residential macrophages and removed by the spleen (Hagens et al., 2007). Additionally, the results also revealed that Chitosan@LT-PLGA C/SNPs can efficiently transport the LT to the brain using intranasal route.

3.12. In-vivo pharmacokinetic study

The pharmacokinetic parameters of prepared NPs after intranasal and intravenous administration are depicted in Fig. 7 and Table 2. The results demonstrated that LT-PLGA NPs and Chitosan@LT-PLGA C/S NPs after intranasal administration showed higher amount of LT in brain as compared to LT-PLGA NPs and Chitosan@LT-PLGA C/S NPs administered intravenously. The results also revealed that intranasally administered LT-PLGA NPs and Chitosan@LT-PLGA C/S NPs showed higher AUC and Cmax in brain as compared to LT-PLGA NPs and Chitosan@LT-PLGA C/S NPs administered intravenously. In addition to this, when LT-PLGA NPs and Chitosan@LT-PLGA C/S NPs administered intranasally, the LT concentration in the brain was higher (Cmax: 41.10 ± 1.97 and 70.30 ± 2.39 and AUC: 464.43 ± 16.71 and 801.18 ± 27.67), respectively as compared to LT concentration (Cmax: 12.70 ± 0.03 and AUC: 143.18 ± 5.19) obtained when LT Suspension administered intranasally. Furthermore, when administered intranasally LT concentration in the brain from LT-PLGA NPs and Chitosan@LT-PLGA C/S NPs was higher as compared to LT-PLGA NPs and Chitosan@LT-PLGA C/SNPs (Cmax: 36.90 ± 1.63 and 59.70 ± 2.25 and AUC: 417.78 ± 17.67 and 676.23 ± 28.99) respectively, when administered intravenously. Similarly, the LT concentration in the brain from Chitosan@LT-PLGA C/SNPs was significantly increased as compared to LT-PLGA NPs. This may be owing to the presence of chitosan over the PLGA NPs, as chitosan enhances the mucoadhesion as well as responsible for opening epithelial tight

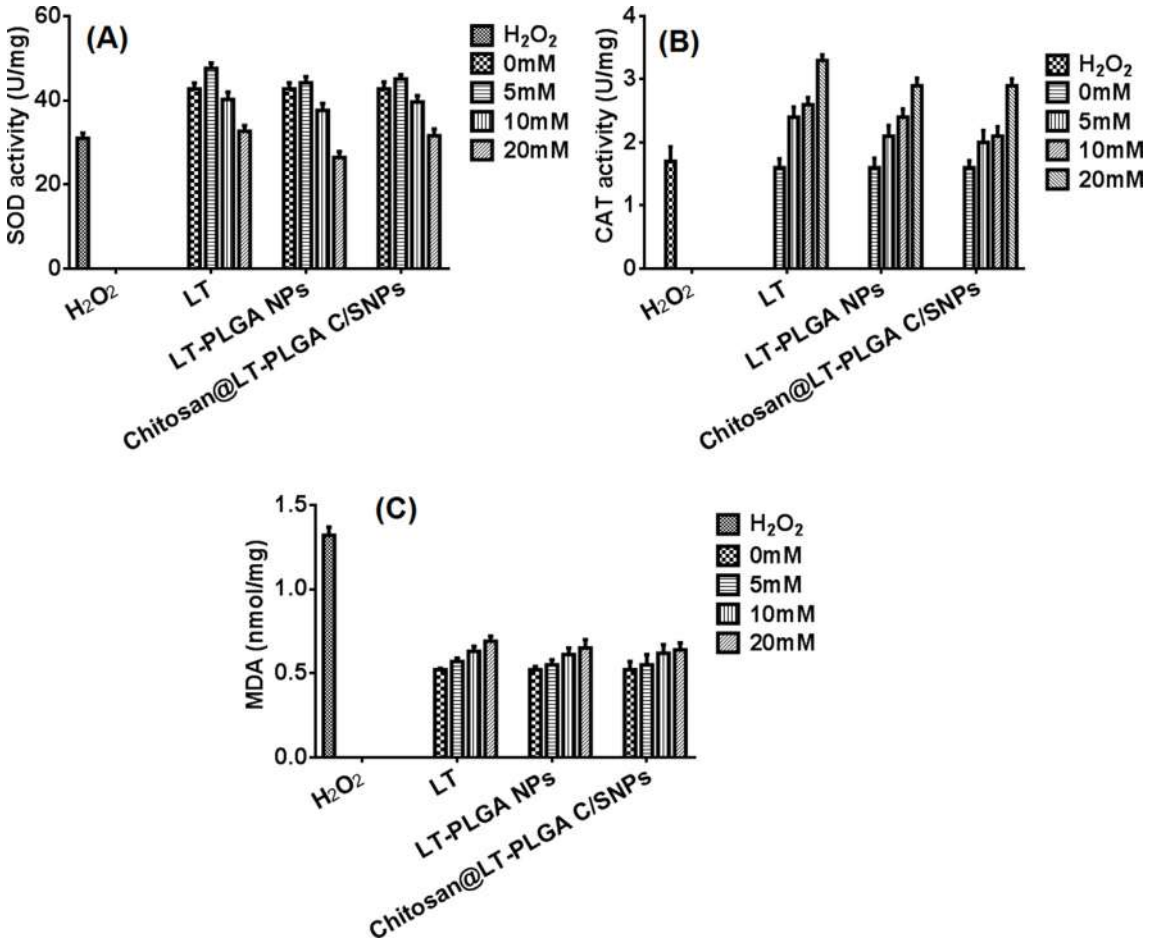

Fig. 5. Antioxidant assay using SOD activity (A); CAT activity (B); and MDA level (C) of pure LT, LT-PLGA NPs and Chitosan@LT-PLGA C/SNPs.

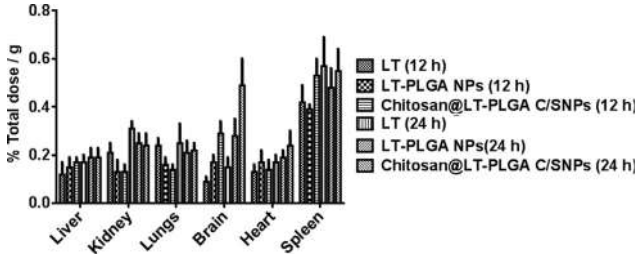

Fig. 6. Bio-distribution study of pure LT, LT-PLGA NPs and Chitosan@LT-PLGA C/SNPs.

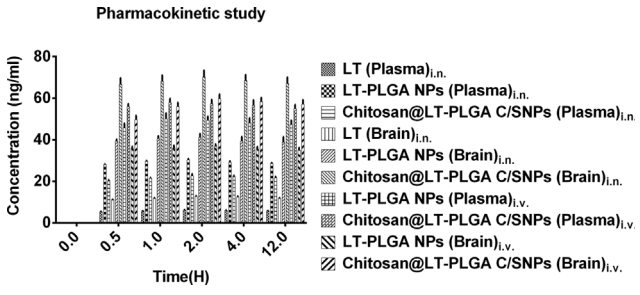

Fig. 7. *In-vivo* pharmacokinetic study of LT-PLGA NPs and Chitosan@LT-PLGA C/SNPs using intranasal and intravenous route and pure LT using intranasal route. The statistical analysis was carried out using one-way ANOVA. P value less than 0.05 was considered significant.

junctions resulting into enhance permeation through nasal mucosa and increase LT concentration in brain (Bhattamisra et al., 2020). Moreover, intranasal administration of LT-PLGA NPs and Chitosan@LT-PLGA C/SNPs showed significant lesser Cmax and AUC in plasma as compared to when LT-PLGA NPs and Chitosan@LT-PLGA C/SNPs when administered intranasally. The results confirmed that intranasal administration of prepared NPs and LT suspension were less expose to circulatory system as compared to NPs administered intravenously. Additionally, the drug targeting efficiency (DTE%) and direct transport percentage (DTP%) was found to be 182.94 ± 10.81; 302.14 ± 14.49 and 45.34 ± 2.03; 66.90 ± 2.73, respectively for LT-PLGA NPs and Chitosan@LT-PLGA C/SNPs and are depicted in Table 3. The results suggested that Chitosan@LT-PLGA C/SNPs showed greater targeting efficiency as compared to LT-PLGA NPs. This can be explained by the valuable properties of chitosan i.e. chitosan can adhere to mucus and increases NPs residence time at the site of absorption resulting and avoid mucociliary clearance. Secondly, chitosan are also responsible for opening of epithelial tight junctions (Bhattamisra et al., 2020; Md et al., 2014). Thus aforementioned results and statements conclude that chitosan can play significant role for targeting LT to the brain following intranasal route. The results obtained are in accordance with Zhang et.al. (Zhang et al., 2013). Zhang et.al revealed that chitosan as a coating material (chitosan coated neurotoxin loaded PLA NPs) (CS-NT-PLA NPs) can enhance the targeting efficiency of drugs as compared to core NPs (NT-PLA NPs). Additionally, both type of NPs demonstrated same Tmax, however, distinct AUC. Thus, the results of present investigation confirm that higher LT can be transported to brain following intranasal administration of Chitosan@LT-PLGA C/SNPs as compared to LT-PLGA NPs and LT suspension.

Table 2
Pharmacokinetic parameters of LT, LT-PLGA NPs and Chitosan@LT-PLGA C/SNPs after intranasal and intravenous administration.

After Intranasal Administration						
Parameter	LT (Plasma)$_{i.n.}$	LT (Brain)$_{i.n.}$	LT-PLGA NPs (Plasma)$_{i.n.}$	LT-PLGA NPs (Brain)$_{i.n.}$	Chitosan@LT-PLGA C/SNPs (Plasma)$_{i.n.}$	Chitosan@LT-PLGA C/SNPs (Brain)$_{i.n.}$
$t_{1/2}$ (h)	129.98 ± 4.37	113.31 ± 3.91	146.63 ± 5.01	158.05 ± 5. 97	165.34 ± 6.29	177.47 ± 7.85
T_{max} (h)	2.00 ± 0.12	2.00 ± 0.2	2.00 ± 0.09	2.00 ± 0.1	2.00 ± 0.17	2.00 ± 0.98
C_{max} (ng/ml)	6.30 ± 0.02	12.70 ± 0.03	30.40 ± 1.1	41.10 ± 1.97	22.70 ± 0.07	70.30 ± 2.39
AUC $_{0-t}$ (ng/ml*h)	70.77 ± 2.13	143.18 ± 5.19	342.78 ± 10.93	464.43 ± 16.71	258.58 ± 10.85	801.18 ± 27.67
MRT $_{0-inf}$ (h)	187.95 ± 7.27	163.86 ± 5.79	211.92 ± 9.2	228.37 ± 8.95	238.91 ± 11.87	256.39 ± 12.03
After Intravenous Administration						
Parameter	LT-PLGA NPs (Plasma)$_{i.v.}$	LT-PLGA NPs (Brain)$_{i.v.}$	Chitosan@LT-PLGA C/SNPs (Plasma)$_{i.v.}$	Chitosan@LT-PLGA C/SNPs (Brain)$_{i.v.}$		
$t_{1/2}$ (h)	151.44 ± 5.69	161.85 ± 6.73	169.80 ± 7.01	176.67 ± 7.75		
T_{max} (h)	1.00 ± 0.03	2.00 ± 0.11	1.00 ± 0.05	2.00 ± 0.09		
C_{max} (ng/ml)	50.10 ± 1.39	36.90 ± 1.63	57.90 ± 2.09	59.70 ± 2.25		
AUC $_{0-t}$ (ng/ml*h)	564.08 ± 21.09	417.78 ± 17.67	659.43 ± 25.71	676.23 ± 28.99		
MRT $_{0-inf}$ (h)	218.87 ± 9.07	233.86 ± 10.02	245.24 ± 9.15	255.31 ± 12.07		

Table 3
DTE% and DTP% of LT-PLGA NPs and Chitosan@LT-PLGA C/SNPs after intranasal administration.

Formulation	%DTE	%DTP
LT-PLGA NPs	182.94 ± 10.81	45.34 ± 2.03
Chitosan@LT-PLGA C/SNPs	302.14 ± 14.49	66.90 ± 2.73

3.13. In-vivo toxicity study

In-vivo toxicity study of prepared NPs was measured by assessing biochemical parameters of blood after intranasal administration in mice. The results demonstrated that no mortality or toxicity related clinical signs were observed in mice after consecutive dosing for 7 days (Table 4). In addition, there were no signs or symptoms of change in behaviour or movement or any toxicity during or post-treatment of 7 days. The results demonstrated that examination of blood with respect to NPs administered groups showed insignificant effect on haematological and biochemical parameter values as compared to control group (Pandey et al., 2020). Thus, it can be concluded that both LT-PLGA NPs and Chitosan@LT-PLGA C/SNPs were safe to be administered via intranasal route.

Table 4
In-vivo toxicity assessment by estimating biochemical parameters after intranasal administration of NPs (LT-PLGA NPs and Chitosan@LT-PLGA C/SNPs) after 7 days.

Parameters	Control	LT-PLGA NPs	Chitosan@LT-PLGA C/SNPs
HB%	13.06 ± 0.42	13.22 ± 0.47	14.90 ± 0.54
RBC *10^3/cmm	8.13 ± 0.81	8.14 ± 0.33	8.17 ± 0.41
WBC*10^3/cmm	8.15 ± 2.31	8.39 ± 0.64	8.17 ± 1.04
PLT*10^5/cmm	5.24 ± 0.47	5.09 ± 0.31	5.09 ± 0.71
N%	51.7 ± 3.15	53.19 ± 3.95	53.21 ± 4.09
E%	0.65 ± 0.07	0.65 ± 0.07	0.69 ± 0.05
L%	31.25 ± 2.81	32.31 ± 3.12	33.72 ± 2.41
M%	0.84 ± 0.04	0.87 ± 0.03	0.87 ± 0.03
PCV%	48.5 ± 5.02	48.3 ± 4.13	48.7 ± 5.14
Bil (mg/dl)	0.35 ± 0.03	0.36 ± 0.03	0.38 ± 0.09
OT (IU/L)	189.2 ± 21.75	194.3 ± 15.4	188.3 ± 20.4
PT (IU/L)	141 ± 24.3	143.5 ± 17.3	147.5 ± 12.9
ALK (IU/L)	132 ± 11.8	132.5 ± 15.1	132.6 ± 18.7
PRO (g/dl)	8.09 ± 1.07	7.90 ± 1.04	7.98 ± 1.17
ALB (g/dl)	3.15 ± 0.47	3.15 ± 0.44	3.15 ± 0.50
GLB (g/dl)	4.39 ± 0.37	4.41 ± 0.22	4.49 ± 0.27
BUN (mg/dl)	11.20 ± 1.31	11.02 ± 1.21	11.17 ± 1.47
CREAT (mg/dl)	1.27 ± 0.42	1.30 ± 0.23	1.34 ± 0.47

3.14. Stability studies

3.14.1. Photostability study

The carotenoid stability is based on various factors such as type of carotenoid, atmospheric oxygen based contact, composition of surfactants, polymer type, polymer concentration. LT stability depends on temperature, oxygen, light, pH and interfacial layer composition (Anarjan and Tan, 2013). LT stability is matter of concern in pharmaceutical and food industries, however, due to presence of isoprenoid holding multiple conjugated double bonds makes lutein unstable (Shi and Chen, 1997). Therefore, photostability study was carried out to compare stability of LT in LT suspension and when incorporated in PLGA NPs and Chitosan@PLGA C/SNPs. The results (Fig. 8A) demonstrated that LT stability in PLGA NPs and CSNPs when exposed to UV was found to be 75.43 ± 0.53% and 84.73 ± 0.09% (% LT retention) which was far greater than that of LT in LT suspension i.e. 9.35 ± 0.61% after 24 h. The results suggest that LT is protected by PLGA NPs and Chitosan@PLGA C/SNPs from external environmental factors. However, Chitosan@LT-PLGA C/SNPs were capable of retaining more amount LT as compared to LT-PLGA NPs which may due to coating of chitosan shell over PLGA NPs.

3.14.2. Thermal stability study

Thermal stability (Chittasupho et al., 2018) of LT-PLGA NPs and Chitosan@LT-PLGA C/SNPs was performed at 4 °C, 25 °C and 30 °C for 30 days by assessing particle size, PDI and surface charge against pure LT suspension. The results demonstrated that both type of NPs were found to be stable when stored at 4 °C, 25 °C and 30 °C. However, it was found that as the temperature increased the average particle size of NPs, particle size distribution was increased and zeta potential was decreased but was not significant. The effect of temperature on particle size, PDI and zeta potential are demonstrated in Fig. 8B, 8C and 8D, respectively. The initial particle size, PDI and surface charge on LT suspension at 4 °C, 25 °C and 30 °C was 498.40 ± 0.10 nm, 0.476 ± 0.009 and −20 ± 1.30 mV, respectively. However, at the end of 30 days, the particle size of LT suspension when stored at 4 °C, 25 °C and 30 °C was found to be 1365.00 ± 2.00 nm, 3592 ± 0.50 nm and 2752.1 ± 2.10 nm, respectively, which revealed the instability of LT in suspension form. At all the exposed temperature PDI showed high polydispersivity of suspension (PDI = 1.00) indicating high particle size distribution in suspension. Surface charge of LT suspension at all exposed temperature was reduced from −20 ± 1.30 mV to low negative i.e. near to −10.60 ± 2.30 mV.

The initial particle size, PDI and surface charge of LT-PLGA NPs at 4 °C, 25 °C and 30 °C was 136.2 ± 0.10 nm, 0.093 ± 0.004and −49.10 ± 1.10 mV, respectively. However, at the end of 30 days, the

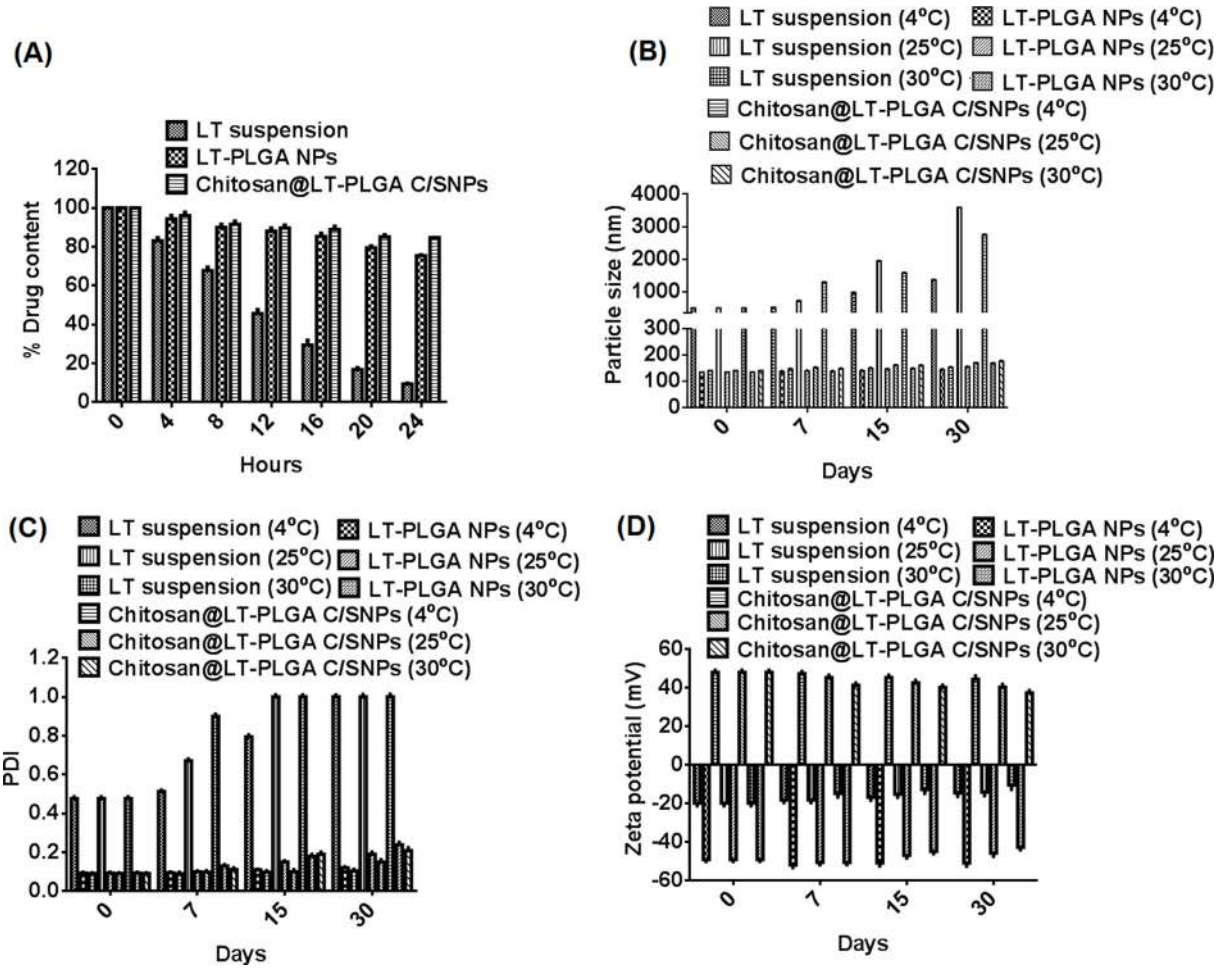

Fig. 8. Photostability study (A) and thermal stability study (B) of pure LT, LT-PLGA NPs and Chitosan@LT-PLGA C/SNPss.

particle size of LT-PLGA NPs when stored at 4 ˚C, 25 ˚C and 30 ˚C was found to be 145.00 ± 1.51 nm, 156 ± 0.50 nm and 169.30 ± 1.34 nm, respectively, which revealed that as temperature increased the particle size of LT-PLGA NPs were also increased. At all the exposed temperature, PDI and surface charge showed insignificant effect indicating colloidal solution of LT-PLGA NPs were uniformly dispersed and stable. The initial particle size, PDI and surface charge on Chitosan@LT-PLGA C/SNPs at 4 ˚C, 25 ˚C and 30 ˚C was 142.30 ± 0.12 nm, 0.091 ± 0.005 and + 47.90 ± 1.11 mV, respectively. However, at the end of 30 days, the particle size of Chitosan@LT-PLGA C/SNPs when stored at 4 ˚C, 25 ˚C and 30 ˚C was found to be 153.70 ± 1.57 nm, 170.80 ± 0.08 nm and 177.00 ± 1.28 nm, respectively, which revealed that as temperature increased the particle size of Chitosan@LT-PLGA C/SNPs were also increased. At all the exposed temperature, PDI and surface charge showed insignificant effect indicating colloidal solution of Chitosan@LT-PLGA C/SNPs were uniformly dispersed and stable. The little reduction in surface charge of Chitosan@LT-PLGA C/SNPs (i.e. from + 47.90 ± 1.11 mV to + 37.20 ± 1.33 mV) can be explained by the fact that chitosan coating till certain extent might have got detached from the surface of PLGA NPs. However, +37.2 indicate the stable colloidal solution of Chitosan@LT-PLGA C/SNPs. The results conclude that prepared LT-PLGA NPs and Chitosan@LT-PLGA C/SNPs showed greater stability at 4 ˚C for a month than that of when stored at 25 ˚C and 30 ˚C.

3.15. Conclusion

In the present investigation, Chitosan@LT-PLGA C/SNPs were fabricated by nanoprecipitation method followed by coating byelectrostatic interaction. The release profile of LT from Chitosan@LT-PLGA C/SNPs exhibited sustained release. Chitosan@LT-PLGA C/SNPs exhibited great ability to cross nasal mucosal membrane as compared to core PLGA NPs and pure LT suspension. The obtained results confirmed that cationic Chitosan@LT-PLGA C/SNPs help in transporting LT to brain via intranasal route and the LT is able to supress the oxidative stress inside the cells. The overall results suggest LT as potential remedy for decreasing oxidative stress while Chitosan@LT-PLGA C/SNPs as efficient carrier and intranasal route as an efficient route for brain targeting of LT in the treatment of AD.

CRediT authorship contribution statement

Namdev Dhas: Conceptualization, Methodology, Software, Data curation, Visualization, Investigation, Writing - original draft. **Tejal Mehta:** Conceptualization, Data curation, Supervision, Writing - review & editing.

Declaration of Competing Interest

The authors declare that they have no known competing financial interests or personal relationships that could have appeared to influence the work reported in this paper.

Acknowledgement

Authors would like to thank Council of Scientific and Industrial Research (CSIR) and Institute of Pharmacy, Nirma University for providing financial assistance in the form of CSIR-SRF (09/1048(007)/2018-EMR-I) and Nirma University (NU/IP/stipend/Ph.D./2016) to Namdev Dhas. The authors are again thankful to Institute of Pharmacy, Nirma University for providing the necessary facilities to carry out the research work.

References

Abruzzo, A., Cerchiara, T., Bigucci, F., Zuccheri, G., Cavallari, C., Saladini, B., Luppi, B., 2019. Cromolyn-crosslinked chitosan nanoparticles for the treatment of allergic rhinitis. Eur. J. Pharm. Sci. 131, 136–145. https://doi.org/10.1016/j.ejps.2019.02.015.

Ahmad, N., Ahmad, R., Alrasheed, R.A., Almatar, H.M.A., Al-Ramadan, A.S., Amir, M., Sarafroz, M., 2020. Quantification and Evaluations of Catechin Hydrate Polymeric Nanoparticles Used in Brain Targeting for the Treatment of Epilepsy. Pharmaceutics 12. https://doi.org/10.3390/pharmaceutics12030203.

Aldawsari, H.M., Alhakamy, N.A., Padder, R., Husain, M., Md, S., 2020. Preparation and Characterization of Chitosan Coated PLGA Nanoparticles of Resveratrol: Improved Stability, Antioxidant and Apoptotic Activities in H1299 Lung Cancer Cells. Coatings 10, 439. https://doi.org/10.3390/coatings10050439.

Alhakamy, N.A., Md, S., 2019. Repurposing Itraconazole Loaded PLGA Nanoparticles for Improved Antitumor Efficacy in Non-Small Cell Lung Cancers. Pharmaceutics 11. https://doi.org/10.3390/pharmaceutics11120685.

Anarjan, N., Tan, C.P., 2013. Effects of Storage Temperature, Atmosphere and Light on Chemical Stability of Astaxanthin Nanodispersions. J Am Oil Chem Soc 90, 1223–1227. https://doi.org/10.1007/s11746-013-2270-8.

Bhattamisra, S.K., Shak, A.T., Xi, L.W., Safian, N.H., Choudhury, H., Lim, W.M., Shahzad, N., Alhakamy, N.A., Anwer, M.K., Radhakrishnan, A.K., Md, S., 2020. Nose to brain delivery of rotigotine loaded chitosan nanoparticles in human SH-SY5Y neuroblastoma cells and animal model of Parkinson's disease. Int. J. Pharm. 579, 119148. https://doi.org/10.1016/j.ijpharm.2020.119148.

Chittasupho, C., Posritong, P., Ariyawong, P., 2018. Stability, Cytotoxicity, and Retinal Pigment Epithelial Cell Binding of Hyaluronic Acid-Coated PLGA Nanoparticles Encapsulating Lutein. AAPS PharmSciTech 20, 4. https://doi.org/10.1208/s12249-018-1256-0.

Cho, E.C., Xie, J., Wurm, P.A., Xia, Y., 2009. Understanding the role of surface charges in cellular adsorption versus internalization by selectively removing gold nanoparticles on the cell surface with a I2/KI etchant. NANO Lett. 9, 1080–1084. https://doi.org/10.1021/nl803487r.

Chuacharoen, T., Sabliov, C.M., 2016. Stability and controlled release of lutein loaded in zein nanoparticles with and without lecithin and pluronic F127 surfactants. Colloids Surf., A 503, 11–18. https://doi.org/10.1016/j.colsurfa.2016.04.038.

Conner, S.D., Schmid, S.L., 2003. Regulated portals of entry into the cell. Nature 422, 37–44. https://doi.org/10.1038/nature01451.

Daverey, A., Agrawal, S.K., 2018. Pre and post treatment with curcumin and resveratrol protects astrocytes after oxidative stress. Brain Res. 1692, 45–55. https://doi.org/10.1016/j.brainres.2018.05.001.

Deepika, D., Dewangan, H.K., Maurya, L., Singh, S., 2019. Intranasal Drug Delivery of Frovatriptan Succinate-Loaded Polymeric Nanoparticles for Brain Targeting. J Pharm Sci 108, 851–859. https://doi.org/10.1016/j.xphs.2018.07.013.

Dhas, N.L., Ige, P.P., Kudarha, R.R., 2015. Design, optimization and in-vitro study of folic acid conjugated-chitosan functionalized PLGA nanoparticle for delivery of bicalutamide in prostate cancer. Powder Technol. 283, 234–245. https://doi.org/10.1016/j.powtec.2015.04.053.

Dhas, N.L., Kudarha, R.R., Mehta, T.A., 2019. Intranasal Delivery of Nanotherapeutics/Nanobiotherapeutics for the Treatment of Alzheimer's Disease: A Proficient Approach. CRT 36. https://doi.org/10.1615/CritRevTherDrugCarrierSyst.2018026762.

Dhas, N.L., Raval, N.J., Kudarha, R.R., Acharya, N.S., Acharya, S.R., 2018. Chapter 9 - Core–shell nanoparticles as a drug delivery platform for tumor targeting, in: Grumezescu, A.M. (Ed.), Inorganic Frameworks as Smart Nanomedicines. William Andrew Publishing, pp. 387–448. https://doi.org/10.1016/B978-0-12-813661-4.00009-2.

do Prado Silva, J.T., Geiss, J.M.T., Oliveira, S.M., Brum, E. da S., Sagae, S.C., Becker, D., Leimann, F.V., Ineu, R.P., Guerra, G.P., Gonçalves, O.H., 2017. Nanoencapsulation of lutein and its effect on mice's declarative memory. Mater Sci Eng C Mater Biol Appl 76, 1005–1011. https://doi.org/10.1016/j.msec.2017.03.212.

Hagens, W.I., Oomen, A.G., de Jong, W.H., Cassee, F.R., Sips, A.J.A.M., 2007. What do we (need to) know about the kinetic properties of nanoparticles in the body? Regul. Toxicol. Pharm. 49, 217–229. https://doi.org/10.1016/j.yrtph.2007.07.006.

Hillaireau, H., Couvreur, P., 2009. Nanocarriers' entry into the cell: relevance to drug delivery. Cell. Mol. Life Sci. 66, 2873–2896. https://doi.org/10.1007/s00018-009-0053-z.

Islam, M.A., Park, T.-E., Reesor, E., Cherukula, K., Hasan, A., Firdous, J., Singh, B., Kang, S.-K., Choi, Y.-J., Park, I.-K., Cho, C.-S., 2015. Mucoadhesive Chitosan Derivatives as Novel Drug Carriers. Curr. Pharm. Des. 21, 4285–4309. https://doi.org/10.2174/1381612821666150901103819.

Karlina, M.V., Pozharitskaya, O.N., Shikov, A.N., Kosman, V.M., Makarova, M.N., Makarov, V.G., 2008. LC Method for Quantification of Lutein in Rat Plasma: Validation, and Application to a Pharmacokinetic Study. Chroma 68, 949–954. https://doi.org/10.1365/s10337-008-0804-2.

Khan, N., Ameeduzzafar, null, Khanna, K., Bhatnagar, A., Ahmad, F.J., Ali, A., 2018. Chitosan coated PLGA nanoparticles amplify the ocular hypotensive effect of forskolin: Statistical design, characterization and in vivo studies. Int. J. Biol. Macromol. 116, 648–663. https://doi.org/10.1016/j.ijbiomac.2018.04.122.

Lin, X., Bai, D., Wei, Z., Zhang, Y., Huang, Y., Deng, H., Huang, X., 2019. Curcumin attenuates oxidative stress in RAW264.7 cells by increasing the activity of antioxidant enzymes and activating the Nrf2-Keap1 pathway. PLoS ONE 14, e0216711. https://doi.org/10.1371/journal.pone.0216711.

Lu, B., Lv, X., Le, Y., 2019. Chitosan-Modified PLGA Nanoparticles for Control-Released Drug Delivery. Polymers (Basel) 11. https://doi.org/10.3390/polym11020304.

Mathur, P., Sharma, S., Rawal, S., Patel, B., Patel, M.M., 2019. Fabrication, optimization, and in vitro evaluation of docetaxel-loaded nanostructured lipid carriers for improved anticancer activity. J Liposome Res 1–15. https://doi.org/10.1080/08982104.2019.1614055.

Md, S., Haque, S., Fazil, M., Kumar, M., Baboota, S., Sahni, J.K., Ali, J., 2014. Optimised nanoformulation of bromocriptine for direct nose-to-brain delivery: biodistribution, pharmacokinetic and dopamine estimation by ultra-HPLC/mass spectrometry method. Expert Opinion on Drug Delivery 11, 827–842. https://doi.org/10.1517/17425247.2014.894504.

Mehta, T.A., Shah, N., Parekh, K., Dhas, N., Patel, J.K., 2019. Surface-Modified PLGA Nanoparticles for Targeted Drug Delivery to Neurons. In: Pathak, Y.V. (Ed.), Surface Modification of Nanoparticles for Targeted Drug Delivery. Springer International Publishing, Cham, pp. 33–71. https://doi.org/10.1007/978-3-030-06115-9_3.

Meng, Q., Wang, A., Hua, H., Jiang, Y., Wang, Y., Mu, H., Wu, Z., Sun, K., 2018. Intranasal delivery of Huperzine A to the brain using lactoferrin-conjugated N-trimethylated chitosan surface-modified PLGA nanoparticles for treatment of Alzheimer's disease. International Journal of Nanomedicine 13, 705–718. https://doi.org/10.2147/IJN.S151474.

Muhoza, B., Zhang, Y., Xia, S., Cai, J., Zhang, X., Su, J., 2018. Improved stability and controlled release of lutein-loaded micelles based on glycosylated casein via Maillard reaction. J. Funct. Foods 45, 1–9. https://doi.org/10.1016/j.jff.2018.03.035.

Mukherjee, S., Ghosh, R.N., Maxfield, F.R., 1997. Endocytosis. Physiol. Rev. 77, 759–803. https://doi.org/10.1152/physrev.1997.77.3.759.

Navarro, S.M., Darensbourg, C., Cross, L., Stout, R., Coulon, D., Astete, C.E., Morgan, T., Sabliov, C.M., 2014. Biodistribution of PLGA and PLGA/chitosan nanoparticles after repeat-dose oral delivery in F344 rats for 7 days. Ther Deliv 5, 1191–1201. https://doi.org/10.4155/tde.14.79.

Paka, G.D., Ramassamy, C., 2017. Optimization of Curcumin-Loaded PEG-PLGA Nanoparticles by GSH Functionalization: Investigation of the Internalization Pathway in Neuronal Cells. Mol. Pharm. 14, 93–106. https://doi.org/10.1021/acs.molpharmaceut.6b00738.

Pandey, A., Singh, K., Patel, S., Singh, R., Patel, K., Sawant, K., 2019. Hyaluronic acid tethered pH-responsive alloy-drug nanoconjugates for multimodal therapy of glioblastoma: An intranasal route approach. Mater. Sci. Eng., C 98, 419–436. https://doi.org/10.1016/j.msec.2018.12.139.

Pandey, A., Singh, K., Subramanian, S., Korde, A., Singh, R., Sawant, K., 2020. Heterogeneous surface architectured pH responsive Metal-Drug Nano-conjugates for mitochondria targeted therapy of Glioblastomas: A multimodal intranasal approach. Chem. Eng. J. 394, 124419. https://doi.org/10.1016/j.cej.2020.124419.

Piazzini, V., Landucci, E., D'Ambrosio, M., Tiozzo Fasiolo, L., Cinci, L., Colombo, G., Pellegrini-Giampietro, D.E., Bilia, A.R., Luceri, C., Bergonzi, M.C., 2019. Chitosan coated human serum albumin nanoparticles: A promising strategy for nose-to-brain drug delivery. Int. J. Biol. Macromol. 129, 267–280. https://doi.org/10.1016/j.ijbiomac.2019.02.005.

Ranganathan, A., Manabe, Y., Sugawara, T., Hirata, T., Shivanna, N., Baskaran, V., 2019. Poly (D, L-lactide-co-glycolide)-phospholipid nanocarrier for efficient delivery of macular pigment lutein: absorption pharmacokinetics in mice and antiproliferative effect in Hep G2 cells. Drug Deliv Transl Res 9, 178–191. https://doi.org/10.1007/s13346-018-0590-9.

Rejman, J., Oberle, V., Zuhorn, I.S., Hoekstra, D., 2004. Size-dependent internalization of particles via the pathways of clathrin- and caveolae-mediated endocytosis. Biochem. J. 377, 159–169. https://doi.org/10.1042/BJ20031253.

Sahoo, S.K., Panyam, J., Prabha, S., Labhasetwar, V., 2002. Residual polyvinyl alcohol associated with poly (D, L-lactide-co-glycolide) nanoparticles affects their physical properties and cellular uptake. J Control Release 82, 105–114. https://doi.org/10.1016/s0168-3659(02)00127-x.

Sawant, K., Pandey, A., Patel, S., 2016. Aripiprazole loaded poly(caprolactone) nanoparticles: Optimization and in vivo pharmacokinetics. Mater. Sci. Eng., C 66, 230–243. https://doi.org/10.1016/j.msec.2016.04.089.

Shah, B., Khunt, D., Misra, M., Padh, H., 2016. Application of Box-Behnken design for optimization and development of quetiapine fumarate loaded chitosan nanoparticles for brain delivery via intranasal route*. Int. J. Biol. Macromol. 89, 206–218. https://doi.org/10.1016/j.ijbiomac.2016.04.076.

Shi, X.-M., Chen, F., 1997. Stability of lutein under various storage conditions. Food / Nahrung 41, 38–41. https://doi.org/10.1002/food.19970410110.

Tang, S., Wang, A., Yan, X., Chu, L., Yang, X., Song, Y., Sun, K., Yu, X., Liu, R., Wu, Z., Xue, P., 2019. Brain-targeted intranasal delivery of dopamine with borneol and lactoferrin co-modified nanoparticles for treating Parkinson's disease. Drug Deliv 26, 700–707. https://doi.org/10.1080/10717544.2019.1636420.

Tzeyung, A. Shak, Md, S., Bhattamisra, S.K., Madheswaran, T., Alhakamy, N.A., Aldawsari, H.M., Radhakrishnan, A.K., 2019. Fabrication, Optimization, and Evaluation of Rotigotine-Loaded Chitosan Nanoparticles for Nose-To-Brain Delivery. Pharmaceutics 11. https://doi.org/10.3390/pharmaceutics11010026.

Venkateswarlu, V., Manjunath, K., 2004. Preparation, characterization and in vitro release kinetics of clozapine solid lipid nanoparticles. J Control Release 95, 627–638. https://doi.org/10.1016/j.jconrel.2004.01.005.

Zhang, Xingguo, Liu, L., Chai, G., Zhang, Xiangyi, Li, F., 2013. Brain pharmacokinetics of neurotoxin-loaded PLA nanoparticles modified with chitosan after intranasal administration in awake rats. Drug Dev Ind Pharm 39, 1618–1624. https://doi.org/10.3109/03639045.2012.727828.